*Graphical Abstract

## Non-edible animal fat

1. $H_2O$, [*R. oryzae*]
2. $H_2O_2$, [N435]
3. $H_2O$, t-BuOH

## *threo*- 9,10 - dihydroxystearic acid

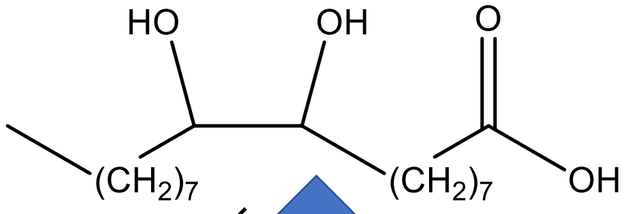


R-OH, [Biocatalyst]
α-Limonene

**Precusor for nylon, lubricants, cosmetics**

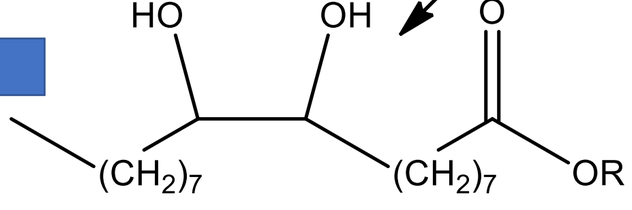


R= $CH_3(CH_2)_n$-

n=0-5,7,9,11,13,15,17

**esters of *threo*- 9,10 – dihydroxystearic acid**

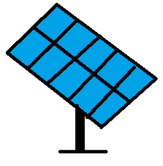



**Sustainable Bio-based PCM**

# Combining biocatalysts to achieve new phase change materials. Application to non-edible animal fat

*Pau Gallart-Sirvent*[a], *Marc Martín*[b], *Aran Solé*[c], *Gemma Villorbina*[a], *Mercè Balcells*[a], *Luisa F. Cabeza**[b], *Ramon Canela-Garayoa*[*,a]

[a] Department of Chemistry-DBA center, University of Lleida, ETSEA, Av. Rovira Roure 191, 25198, Lleida, Spain

[b] GREA Innovació concurrent, INSPIRES Research Centre, University of Lleida, Pere de Cabrera s/n, 25001, Lleida, Spain

[c] Department of Mechanical Engineering and Construction, Universitat Jaume I, Campus del Riu Sec s/n, 12071 Castelló de la Plana, Spain

*Corresponding authors:

canela@quimica.udl.cat and lcabeza@diei.udl.cat

ABSTRACT: The thermal properties of various alkyl *threo*-9, 10-dihydroxystearates (DHSEs) prepared from non-edible fat were studied. Non-edible animal fat was hydrolyzed in a 93% yield with *R. oryzae* resting cells. Crude unsaturated fatty acids were recovered from the matter liquor resulting from a crystallization performed to achieve the saturated fatty acids. These unsaturated free fatty acids were epoxidized with 30% $H_2O_2$ using immobilized *Candida antarctica* Lipase-B

(CAL-B) as biocatalyst. The epoxy ring was cleaved with hot water in the presence of *tert*-butanol (*t*-BuOH). Pure *threo*-9, 10-dihydroxystearic acid (DHSA) from animal fat was recovered by crystallization (51% yield). Subsequently, DHSA was esterified in α-limonene using biocatalysts yielding twelve DHSEs (58-90% yield). Differential scanning calorimetry (DSC) analysis of these esters revealed potential latent heats ranging from 136.83 $kJ \cdot kg^{-1}$ to 234.22 $kJ \cdot kg^{-1}$ and melting temperatures from 52.45 ºC to 76.88 ºC. Finally, the compounds with enthalpies above 200 $kJ \cdot kg^{-1}$ were subjected to 100 and 1000 thermal cycles. These experiments showed that these products present good thermal reliability.

*Keywords:* bioeconomy, bio-based PCM, *threo*-9, 10-dihydroxystearic acid synthesis, α-limonene, fatty acids.

*Abbreviations: t*-BuOH, *tert*-butanol, CAL-B, *Candida antarctica* Lipase-B; DHSA, *threo*-9, 10-dihydroxystearic acid; DHSE, *threo*-9, 10-dihydroxystearate; DHW, domestic hot water; DSC, differential scanning calorimetry; GC-FID, gas chromatography-flame ionization detector; $^{1}H$ NMR, proton nuclear magnetic resonance; IWH, industrial waste heat; PCM, phase change material.

## 1. Introduction

It has been estimated that the world population will reach 9.2 billion by 2050 [1]. Such growth will bring with it a significant increase in livestock production and animal by-products. In this regard, by-products account for almost 60% of the body weight of a farm animal, while 20% corresponds to non-edible ones. Furthermore, dead and fallen animals increase the amount of non-edible by-products. In this scenario, the reuse of non-edible by-products gains increasing

relevance given the public health concerns associated with the non-utilization of such products [2]. Fatty non-edible animal parts comprise mainly triacylglycerides, which contain saturated and unsaturated fatty acids and glycerol. These fats are an interesting source to prepare biodiesel [3] and recently they have been used to prepare bio-based phase change materials (PCMs) [4].

PCMs have the capacity to store heat energy during the phase-change that occurs during melting and solidification processes. In this regard, fatty acids present high thermal and chemical stability and high heat capacity [5,6]. In addition, fatty acids and their derivatives are an excellent source of renewable materials, providing alternatives to currently predominant PCMs such as paraffin and salts [7,8]. Commercially available fatty acid derivatives have recently been proposed as bio-based organic PCMs. These products result from the partial hydrogenation of soy-wax [9,10] or from the hydrogenation of unsaturated triacylglycerides [11-14]. These approaches allow the substitution of paraffin; however, the use of edible oil raises concerns about the likely surplus of food that might cause starvation, especially in the developing countries [15]. Furthermore, although hydrogenation promotes stability during phase change cycles with no risk of oxidation [12,13], the conversion of unsaturated fatty acids to saturated fatty acids circumvents the opportunity of using them for other potential applications.

The unsaturated moieties in fatty acids play an important role in the synthesis of monomers and polymers. The epoxy fatty acid derivatives produced from unsaturated oils allow the formation of pressure-sensitive adhesives (PSAs) [16,17], rubbers [18], coatings[18], polyurethanes [18], and acrylate resins [18]. In addition, oleic acid can be converted to DHSA and cleaved in an oxidative manner to azelaic acid in a green and efficient gold-catalyzed system [19,20]. DHSA has recently been used as starting material for the preparation of lubricants [21], soaps [22], deodorant sticks [22], and shampoos [22]. Nevertheless, common lab-scale syntheses of DHSA

from commercial oleic acid usually involve the use of chemicals, including formic acid, NaOH and HCl [23] or $MgSO_4$, $Na_2SO_3$ and hexane [19]. Additionally, DHSA preparation from palm oil-based oleic acid has recently been patented using conventional chemistry [24] in a moment that palm industry is causing concerns in deforestation and affects in biodiversity [25-27].

Recently, we described a procedure using conventional chemistry to transform non-edible animal fat into palmitic-stearic acid eutectic mixtures and DHSA. These products were also analyzed by DSC analysis with distinct behavior, on the one hand, palmitic-stearic acid eutectic mixtures shown good thermal properties, whereas that DHSA presented low chemical stability, presumably caused by the formation of estolides between the diol and fatty acid moieties [4]. In order to afford PCMs from DHSA, the esterification of DHSA into alkyl *threo*-9, 10-dihydroxystearates (DHSEs) should prevent the estolide formation during DSC analysis. Additionally, fatty acid esters have been widely studied as PCMs [28-33] lowering the corrosive action, bad odor and sublimation showed by fatty acids during heating process. Nevertheless, an acid catalyzed or under vacuum esterification of DHSA could also yield estolides. On the other hand, enzymatic esterifications of DHSA present an excellent selectivity towards DHSEs [34,35].

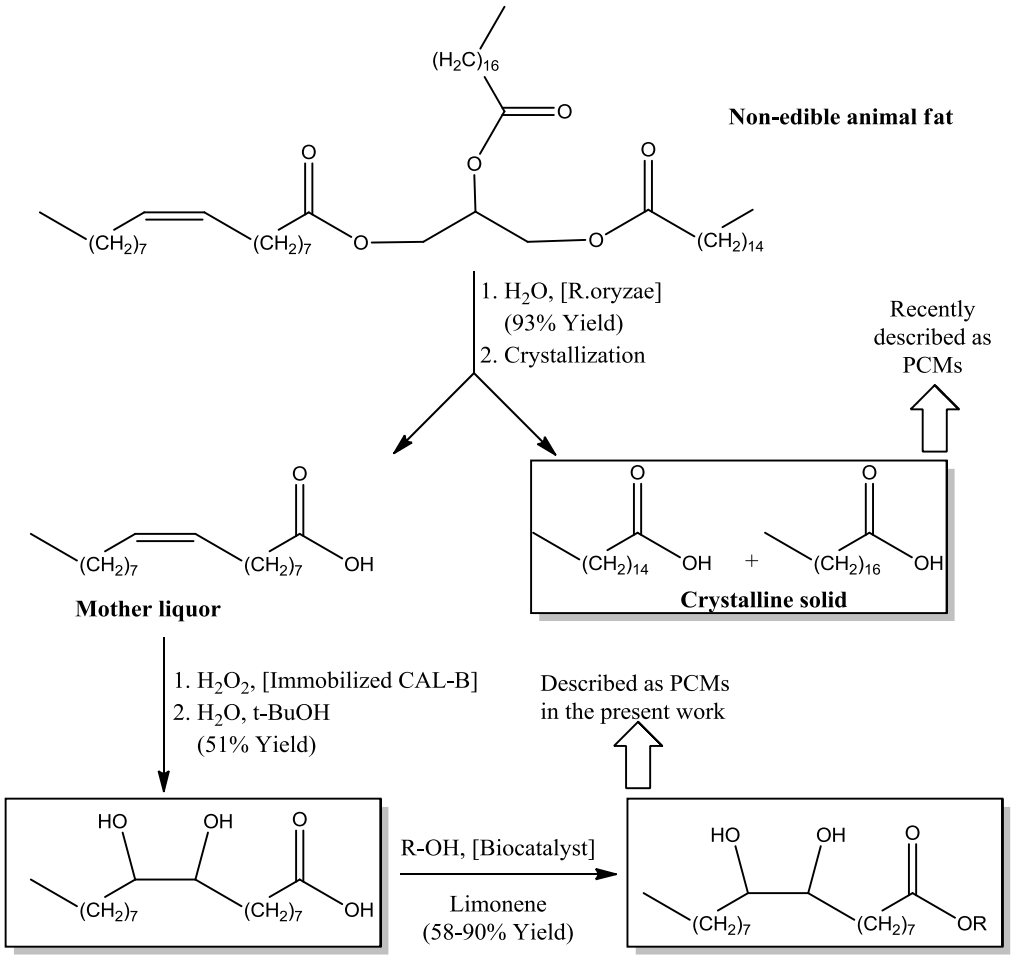


**Figure 1**. Syntheses performed in this study. The triacylglyceride structure shows the three main fatty acids present in fat materials.

The aim of the present work was to combine biocatalytic reactions to prepare new PCMs (**Figure 1)** from non-edible animal fat. First at all, the epoxidation using immobilized CAL-B in a solvent-free media and the epoxide opening with hot water were studied in commercial oleic acid. Subsequently, the non-edible animal fat was hydrolyzed using a bio-catalytic procedure recently described [36], and the crude free acids were split into saturated and unsaturated fatty acids. The unsaturated fatty acids yielded DHSA in the conditions previously studied with

commercial oleic acid. Twelve DHSEs were prepared from DHSA and the corresponding alcohol using immobilized CAL-B as biocatalyst and α-limonene as solvent. DSC was used to test the performance of these esters as PCMs.

## 2. Materials and methods

### *2.1. Materials*

Methanol (≥99.9%), 1-butanol (≥99.5%), 1-dodecanol (98%), 1-hexanol (98%), and oleic acid (90%) were purchased from Sigma-Aldrich Corp. (St. Louis, USA). Ethanol (≥99.9%) was purchased from Scharlau (Barcelona, Spain). 1-Propanol (≥99.8%), 1-pentanol (99%), 1-decanol (97%), 1-tetradecanol (97%), and 1-hexadecanol (99%) were supplied by Fluka (Buchs, Switzerland). 1-Octadecanol (97%) was purchased from Alfa Aesar (Karlsruhe, Germany). 1-Octanol (99%) was purchased from Acros (New Jersey, USA). Hydrogen peroxide (30%) (w/v) solution was provided by Fischer Scientific UK (Leicester, UK). $CO_2$ was obtained from Messer Iberica de Gases S.A (Tarragona, Spain). *Rhizopus oryzae* resting cells were prepared as described by Gallart-Sirvent et al. [36]. Immobilized lipase-B from *C. antarctica* (Novozym® 435) was a gift sample from Novozymes A/S (Bagsvaerd, Denmark). α-Limonene was a kind gift from Creaciones Aromaticas Industriales (Sant Quirze del Vallès, Spain). Animal fat was a kind gift from Subproductos Cárnicos Echevarria y Asociados S.L (Cervera, Spain). The fat was composed of non-edible fatty parts of pig and chicken origin and comprised mainly triglycerides. Composition (GC-FID [37]): Oleic acid (36.97%), linoleic acid (14.64%), stearic acid (14.05%) and palmitic acid (24.57%).

*2.2 Analyses*

$^{1}$H NMR spectra were recorded with a MERCURY plus NMR Spectrometer Systems VARIAN AS 400 MHz magnet. Thermophysical characterization was performed with an 822e differential scanning calorimeter from Mettler Toledo in order to analyze the phase-change temperature and enthalpies (melting and solidification). Two samples of each material were analyzed to ensure repeatability of the results. Measurements were performed at 0.5 ºC•min$^{-1}$ under nitrogen gas at a flow rate of 80 mL•min$^{-1}$. The differential scanning calorimetry (DSC) analyses were performed between 40 ºC and 80 ºC. Around 5 mg of sample was placed into 40-µL aluminum crucibles. The equipment has an accuracy of ± 0.1 ºC for temperature and ±3 kJ•kg$^{-1}$ for enthalpy results.

To study thermal cycling reliability, a Bioer Gene Q T-18 thermal cycler was used to analyze the changes of the phase-change temperature and latent heat of the esters after 100 and 1000 thermal cycles. A 0.5-mL vial was used for each compound. A dynamic method was established using a temperature range between 30 ºC and 95 ºC and at 4 ºC•s$^{-1}$ for cooling and 5 ºC•s$^{-1}$ for heating. A total of 1000 cycles were performed under the described conditions. Finally, the compounds were tested again by DSC to identify changes in their thermophysical properties.

*2.3. Reactions performed with commercial oleic acid*

*2.3.1. Enzymatic epoxidation of oleic acid – Reuse study using* supercritical $CO_2$

A volume of 5.42 mL (47.81 mmol) of a 30% $H_2O_2$ solution (4 ºC) was added to a 50-mL Falcon® Conical Centrifuge tube containing 10 g (31.86 mmol of double bonds) of 90% oleic acid and 1 g of immobilized CAL-B. The vial was fixed horizontally in a Labnet 211DS orbital oven and then shaken at 220 rpm at 55 ºC for 150 min. It was then centrifuged at 6000 rpm for 5 min, and the non-aqueous and aqueous phases were separated. Immobilized CAL-B was recovered by filtering the crude mixture through a Pyrex crucible nº3, washing with water, and

drying the biocatalyst under vacuum for 24 h. Finally, the biocatalyst was extracted with a lab-scale supercritical fluid extractor (Speed SFE-Applied separations). The extraction vessel was packed with the immobilized CAL-B recovered. The extraction temperature, pressure, $CO_2$ outflow rate, and residence time were set at 60°C, 35 MPa, 4 L•min$^{-1}$, and 45 min, respectively. The epoxide recovered from the supercritical $CO_2$ extraction was added to the non-aqueous layer previously obtained. The washed immobilized CAL-B was recovered for a reuse study. The crude product of the reaction was analyzed by $^1$H NMR (see **SI**) spectroscopy after each reuse.

*cis*-9,10-Epoxystearic acid: $^1$H NMR (400 MHz, $CDCl_3$) δ ppm: 0.88 (t, J=6.9 Hz, C**H$_3$**), 1.19-1.55 (m, C**H$_2$**), 1.63 (m, β**CH$_2$**), 2.34 (t, J=7.4 Hz, α**CH$_2$**), 2.90 (m, **H**COC**H**).

*2.3.2. Enzymatic epoxidation of oleic acid – Reusing studies using common organic solvents*

A volume of 542 μL (4.78 mmol) of a 30% $H_2O_2$ solution (4 ºC) was added to a 15-mL Falcon® Conical Centrifuge tube containing 1 g (3.19 mmol) of 90% oleic acid and 0.1 g of immobilized CAL-B. The reaction was performed as described above. The final mixture was then extracted twice with 5 mL of solvent (**Figure 3** shows all the solvents used). Immobilized CAL-B was recovered by filtering the mixture through a Pyrex crucible nº3. The biocatalyst was used for a new solvent-free reaction, and the remaining activity of immobilized CAL-B was evaluated. An aliquot of this new reaction was analyzed by $^1$H NMR spectroscopy. The ratio between the integration value of the signal at 5.10 ppm (**H**C=C**H)** and the signal at 0.88 ppm (C**H$_3$)** in the $^1$H NMR spectra was determined in each experiment. These values were compared with the same ratio at the starting material.

*2.3.3. Preparation of DHSA*

A volume of 5.42 mL (47.81 mmol) of a 30% $H_2O_2$ solution (4 ºC) was added to a 50-mL Falcon® Conical Centrifuge tube containing 10 g (31.86 mmol of double bonds) of 90% oleic acid and 1 g of immobilized CAL-B. The tube was fixed horizontally in a Labnet 211DS orbital oven and shaken at 220 rpm at 55 ºC for 150 min. The crude epoxide was recovered by extracting the final reaction mixture twice with 25 mL of *t*-BuOH. This organic solution was placed in a 150-mL reaction vial containing 50 mL of water. The vial was closed and stirred magnetically in an oil bath at 130 ºC for 12 h. It was then cooled to room temperature and the content was placed in a funnel. The aqueous phase was discarded, and the organic phase was chilled at 4 ºC for 24 h. The final solid was recovered using a Pyrex crucible nº3 and washing three times with cold ethyl acetate (5.50 g, 55% isolated yield). The final white powder (m.p. 94.2 ºC) [38] was analyzed by $^1$H NMR (see **SI**):

$^1$H NMR (400 MHz, $CDCl_3$) δ ppm: 0.88 (t, J=6.9 Hz, C**H$_3$**), 1.19 - 1.55 (m, C**H$_2$**), 1.63 (m, β**CH$_2$**), 2.34 (t, J=7.4 Hz, αC**H$_2$**), 3.40 (m, **H**COH).

*2.4. Preparation of DHSEs from non-edible fat*

*2.4.1. Bio-catalytic hydrolysis of non-edible fat*

The bio-catalytic hydrolysis of the fat and the separation of the resulting free fatty acids by crystallization was performed following the procedure already described [36]. Thus, we added 20 g of water to each 50-mL Falcon® Conical Centrifuge tube (six in total) each containing 20 g of animal fat and 2 g of *Rhizopus oryzae* resting cells. The vials were fixed horizontally in a Labnet 211DS orbital oven and shaken at 220 rpm at 40 ºC for 48 h. Finally, they were centrifuged at 6000 rpm for 10 min, and the non-aqueous and aqueous phases were separated. The resting cells

were recovered using a Pyrex crucible nº3 and then washed with water. The resting cells were dried under vacuum for 24 h. They were then extracted with a lab-scale supercritical fluid extractor (Speed SFE-Applied separations). The extraction temperature, pressure, $CO_2$ outflow rate, and residence time were set at 40°C, 35 MPa, 4 L•min$^{-1}$, and 45 min, respectively. The remaining fatty matter recovered from the supercritical $CO_2$ extraction of the biocatalyst was joined to the non-aqueous phase previously obtained. The resulting non-aqueous viscous liquid (113.58 g, 93% yield) was titrated in duplicate to determine the degree of hydrolysis [36] of the fatty matter (95% of hydrolysis degree). The fatty matter was crystallized with ethanol 1/6 (w/v) at -20 ºC for 24 h. The mother liquor was concentrated, yielding 81.84 g of a highly unsaturated fatty acid mixture. Composition (GC-FID [37]): Oleic acid (55.14%), linoleic acid (30.17%), stearic acid (7.57%) and palmitic acid (6.80%).

*2.4.2. Preparation of DHSA*

A volume of 7 mL (61.74 mmol) of a 30% $H_2O_2$ solution (at 4 ºC) was added to a 50-mL Falcon® Conical Centrifuge tube containing 10 g (41.02 mmol of double bonds) of the highly unsaturated fatty acid mixture and 1 g of immobilized CAL-B. The whole process was performed as described above until the *t*-BuOH solution was achieved. The organic phase was concentrated under vacuum. The final residue was dissolved in hot ethyl acetate in a solute/solvent ratio 1/1 (w/v). The organic mixture was dried over $Na_2SO_4$, filtered and kept at 4 ºC for 24 h. The solid was recovered by filtration using a Pyrex crucible nº3 and washed three times with cold ethyl acetate. The solid was recrystallized in ethyl acetate at 4 ºC in a solute/solvent ratio 1/5 (w/v) to yield 3.13 g of DHSA (51% yield). The reaction was repeated until enough starting material was obtained for further enzymatic esterification reactions. The final white powder (m.p. 93.8 ºC) [38] was analyzed by $^1$H NMR (see **SI**):

$^1$H NMR (400 MHz, $CDCl_3$) δ ppm: 0.88 (t, J=6.9 Hz, C**H$_3$**), 1.19 - 1.55 (m, C**H$_2$**), 1.63 (m, β**CH$_2$**), 2.34 (t, J=7.4 Hz, αC**H$_2$**), 3.40 (m, **H**COH).

*2.4.3. Biocatalytic preparation of octyl DHSE- Reuse study*

A volume of 1 mL of octanol (6.32 mmol) was added to a 15-mL Falcon® Conical Centrifuge tube containing 1 g (3.16 mmol) of DHSA from non-edible animal fat, 100 mg of biocatalyst and 10 mL of α-limonene. The Falcon® Conical Centrifuge tube was fixed horizontally in a Labnet 211DS orbital oven and shaken at 220 rpm at 40 ºC for 24 h. The vial was centrifuged at 6000 rpm for 1 min, and the organic layer was separated from the biocatalyst. This layer was added to another 15-mL Falcon® Conical Centrifuge vial and incubated in the orbital oven at 40 ºC for 5 min (220 rpm) with 3 mL of a saturated solution of $NaHCO_3$. The vial was centrifuged at 6000 rpm for 1 min and α-limonene was recovered. The solid ester appeared when α-limonene was kept at 4 ºC for 24 h. The crystals were recovered by filtration and washing three times with cold α-limonene using a Pyrex crucible nº3. The Falcon® Conical Centrifuge tube containing the biocatalyst was used to repeat the reaction for the reuse study. Experiments were performed in duplicate. The final white powder was analyzed by $^1$H NMR (see **SI**):

$^1$H NMR (400 MHz, $CDCl_3$) δ ppm: 0.88 (t, J=6.9 Hz, C**H$_3$**), 1.19 - 1.55 (m, C**H$_2$**), 1.63 (m, β**CH$_2$**), 1.83-1.93 (s, **H**O-), 2.29 (t, J=7.4 Hz, αC**H$_2$**), 3.40 (m, **H**COH), 4.05 (t, J= 6.7 Hz, C**H$_2$**-O).

*2.4.4. Bio-catalytic preparation of DHSEs: Esters from methanol to 1-tetradecanol (procedure A). Esters of 1-hexadecanol and 1-octadecanol (procedure B)*

A given amount of alcohol (**Table 1**) was added to a 15-mL (A) or 50-mL (B) Falcon® Conical Centrifuge tube containing 1 g (3.16 mmol) of DHSA from non-edible animal fat, 100 mg of immobilized CAL-B, and 10 mL (A) or 20 mL (B) of α-limonene. The reaction conditions were

the described above. Subsequently, 5 mL of methanol (B) and 3 mL of a saturated solution of $NaHCO_3$ (A and B) were added to each vial, which was stirred at 200 rpm at 40 ºC for 5 min (A) or 2 min (B). The vials were centrifuged at 6000 rpm for 1 min and the organic layer was recovered. The solutions were crystallized at various temperatures depending on the ester (**Table 1**). Note that 1-octanyl to 1-octadecanyl esters easily crystallized from α-limonene solutions at room temperature. The crystals of each ester were recovered on a Pyrex crucible nº3 and washed three times with cold α-limonene. **Table 1** shows the isolated yields of the esters synthesized. The esters were analyzed by $^1$H NMR (see **SI**):

**Methyl DHSE:** $^1$H NMR (400 MHz, $CDCl_3$) δ ppm: 0.89 (t, J=6.9 Hz, C**H$_3$**), 1.21-1.55 (m, C**H$_2$**), 1.63 (m, β**CH$_2$**), 2.10-2.27 (s, **H**O-), 2.31 (t, J=7.5 Hz, α**CH$_2$**), 3.40 (m, **H**COH), 3.67 (s, C**H$_3$**-O). **Ethyl DHSE:** $^1$H NMR (400 MHz, $CDCl_3$) δ ppm: 0.86 (t, J=6.8 Hz, C**H$_3$**), 1.17-1.52 (m, C**H$_2$**), 1.60 (m, β**CH$_2$**), 2.27 (t, J=7.5 Hz, α**CH$_2$**), 3.38 (m, **H**COH), 4.11 (q, J= 7.1 Hz, C**H$_2$**-O). **Propyl DHSE:** $^1$H NMR (400 MHz, $CDCl_3$) δ ppm: 0.87 (t, J=6.8 Hz, C**H$_3$**), 0.93 (t, J=7.4 Hz, C**H$_3$**), 1.18-1.52 (m, C**H$_2$**), 1.62 (m, β**CH$_2$**), 2.10-2.24 (s, **H**O-), 2.28 (t, J=7.5 Hz, α**CH$_2$**), 3.38 (m, **H**COH), 4.01 (t, J= 6.7 Hz, C**H$_2$**-O). **Butyl DHSE:** $^1$H NMR (400 MHz, $CDCl_3$) δ ppm: 0.87 (t, J=6.8 Hz, C**H$_3$**), 0.92 (t, J=7.4 Hz, C**H$_3$**), 1.19-1.55 (m, C**H$_2$**), 1.60 (m, β**CH$_2$**), 2.07-2.24 (s, **H**O-), 2.28 (t, J=7.5 Hz, α**CH$_2$**), 3.38 (m, **H**COH), 4.05 (t, J= 6.7 Hz, C**H$_2$**-O). **Pentyl DHSE:** $^1$H NMR (400 MHz, $CDCl_3$) δ ppm: 0.84-0.93 (m, C**H$_3$**), 1.20-1.52 (m, C**H$_2$**), 1.61 (m, β**CH$_2$**), 2.07-2.20 (s, **H**O-), 2.28 (t, J=7.5 Hz, α**CH$_2$**), 3.38 (m, **H**COH), 4.05 (t, J= 6.8 Hz, C**H$_2$**-O). **Hexyl DHSE:** $^1$H NMR (400 MHz, $CDCl_3$) δ ppm: 0.84-0.91 (m, C**H$_3$**), 1.20-1.52 (m, C**H$_2$**), 1.60 (m, β**CH$_2$**), 2.12-2.22 (s, **H**O-), 2.28 (t, J=7.5 Hz, α**CH$_2$**), 3.38 (m, **H**COH), 4.04 (t, J= 6.8 Hz, C**H$_2$**-O). **Octyl DHSE:** $^1$H NMR (400 MHz, $CDCl_3$) δ ppm: 0.87 (t, J=6.7 Hz, C**H$_3$**),

1.18-1.52 (m, C**H**$_2$), 1.60 (m, β**C**H$_2$), 2.03-2.20 (s, **H**O-), 2.28 (t, J=7.5 Hz, αC**H**$_2$), 3.39 (m, **H**COH), 4.04 (t, J= 6.7 Hz, C**H**$_2$-O). **Decyl DHSE:** $^1$H NMR (400 MHz, $CDCl_3$) δ ppm: 0.87 (t, J=6.7 Hz, C**H**$_3$), 1.18-1.52 (m, C**H**$_2$), 1.59 (m, β**C**H$_2$), 2.06-2.16 (s, **H**O-), 2.28 (t, J=7.5 Hz, αC**H**$_2$), 3.38 (m, **H**COH), 4.04 (t, J= 6.7 Hz, C**H**$_2$-O). **Dodecyl DHSE:** $^1$H NMR (400 MHz, $CDCl_3$) δ ppm: 0.87 (t, J=6.8 Hz, C**H**$_3$), 1.18-1.52 (m, C**H**$_2$), 1.61 (m, β**C**H$_2$), 2.04-2.20 (s, **H**O-), 2.28 (t, J=7.5 Hz, αC**H**$_2$), 3.38 (m, **H**COH), 4.04 (t, J= 6.7 Hz, C**H**$_2$-O). **Tetradecyl DHSE:** $^1$H NMR (400 MHz, $CDCl_3$) δ ppm: 0.87 (t, J=6.9 Hz, C**H**$_3$), 1.20-1.52 (m, C**H**$_2$), 1.61 (m, β**C**H$_2$), 1.87-1.97 (s, **H**O-), 2.28 (t, J=7.5 Hz, αC**H**$_2$), 3.37 (m, **H**COH), 4.05 (t, J= 6.8 Hz, C**H**$_2$-O). **Hexadecyl DHSE:** $^1$H NMR (400 MHz, $CDCl_3$) δ ppm: 0.87 (t, J=6.8 Hz, C**H**$_3$), 1.18-1.52 (m, C**H**$_2$), 1.61 (m, β**C**H$_2$), 1.87-1.95 (s, **H**O-), 2.28 (t, J=7.5 Hz, αC**H**$_2$), 3.39 (m, **H**COH), 4.05 (t, J= 6.8 Hz, C**H**$_2$-O). **Octadecyl DHSE:** $^1$H NMR (400 MHz, $CDCl_3$) δ ppm: 0.87 (t, J=6.9 Hz, C**H**$_3$), 1.18-1.52 (m, C**H**$_2$), 1.60 (m, β**C**H$_2$), 1.98-2.06 (s, **H**O-), 2.28 (t, J=7.5 Hz, αC**H**$_2$), 3.39 (m, **H**COH), 4.05 (t, J= 6.8 Hz, C**H**$_2$-O).

**Table 1.** Synthetic specifications of the DHSEs prepared from non-edible animal fat.

| Alkyl DHSE | Isolated Yield (%) | Molar ratio alcohol: DHSA | Crystallization temperature (ºC) |
|---|---|---|---|
| Methyl | 72 | 3:1 | -20 |
| Ethyl | 75 | 3:1 | -20 |
| Propyl | 74 | 3:1 | -20 |
| Butyl | 60 | 5:1 | -20 |
| Pentyl | 77 | 3:1 | -20 |
| Hexyl | 69 | 2:1 | -20 |
| Octyl | 60 | 2:1 | -20 |
| Decyl | 70 | 2:1 | -20 |
| Dodecyl | 79 | 2:1 | -20 |
| Tetradecyl | 90 | 2:1 | 4 |
| Hexadecyl | 90 | 2:1 | 4 |
| Octadecyl | 58 | 1.1:1 | 25 |

## 3. Results and discussions

### *3.1. Study of the reactions applied to commercial oleic acid*

#### *3.1.1. Enzymatic epoxidation of commercial oleic acid*

Enzymatic epoxidations were performed in Falcon® Conical Centrifuge tubes. These vials have already used for the biocatalytic hydrolysis of non-edible animal fat showing a good performance [36]. The use of such vials facilitates the separation of product and biocatalyst by

centrifugation at the end of the reaction. Furthermore, 30% hydrogen peroxide can be added to the reaction mixture at 4 ºC in one step, completing the reaction in 150 min. The combination of the non-aqueous layer and the extracted product permits the achievement of the final yield. Additionally, this extraction methodology allows the reuse of the biocatalyst. **Figure 2** shows the yields of the epoxidation procedure in five consecutive reaction cycles extracting the biocatalyst with supercritical $CO_2$. Epoxide purity was determined by $^1$H NMR [17], comparing the integration value of the signal at 2.34 ppm corresponding to αC**H**$_2$ versus the signal at 2.90 ppm corresponding to the **H**COC**H** protons of the epoxide group. The enzyme catalyzed the full conversion of oleic acid during the first (R0) and second (R1) cycles. Unfortunately, the yield decreased dramatically from the third cycle (R2) onwards presumably regarding to the deactivation of the biocatalyst by highly reactive species such as peroxy/epoxy groups or hydrogen peroxide. Nevertheless, this procedure allows the repetition of the reaction once with the same biocatalyst achieving a full oleic acid conversion and allowing the recovery of the product. In addition, supercritical $CO_2$ meets the requirements of extract and reuse the biocatalyst.

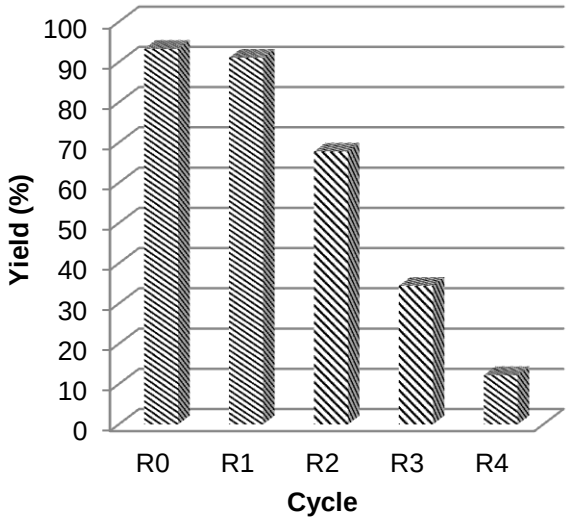


**Figure 2**. Epoxidation yields of commercial oleic acid at 55 ºC for 150 min in a solvent-free medium using immobilized CAL-B as biocatalyst. Data correspond to five experiments using supercritical $CO_2$ for the biocatalyst extraction after each reaction.

To widen the scope of the enzymatic epoxidation study, the immobilized CAL-B was extracted with several organic solvents including α-limonene, instead of using supercritical $CO_2$. Subsequently, the reaction was repeated with the washed biocatalyst. Indeed, an aliquot from the epoxide of the second cycle reaction (R1) was analyzed by $^1$H NMR. As the biocatalyst of that second cycle reaction was not extracted, the total mass of product was not known. Thus, the results are shown in terms of oleic acid conversion. **Figure 3** shows oleic acid conversion on the first reuse (R1) of immobilized CAL-B. The extraction of immobilized CAL-B with non-polar solvents such as α-limonene or hexane resulted in higher retention of the initial activity than that extracted with acetone, ethyl acetate, or *t*-BuOH. The oleic acid conversion of α-limonene (98%) and hexane (95%) sets gave promising results. Nevertheless, hexane is classified as hazardous and the substitution of this sort of solvents is a priority [39].

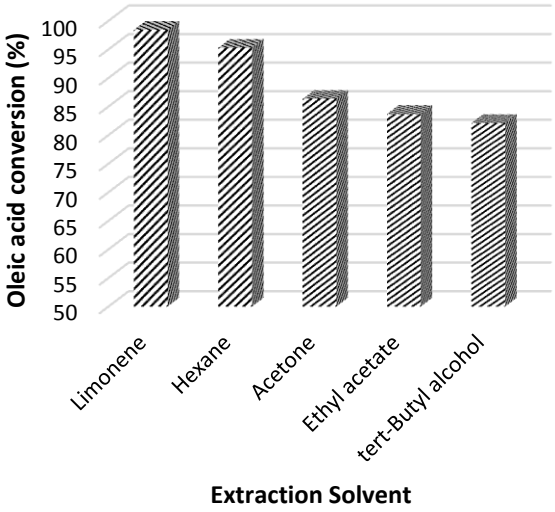


**Figure 3**. Oleic acid epoxidation on the first reuse (R1) of immobilized CAL-B on the epoxidation of commercial (90%) oleic acid at 55 ºC for 150 min in a solvent-free medium.

*3.1.2. Preparation of DHSA from cis-9, 10-epoxystearic acid*

Each solution resulting from the first epoxidation trial with the various solvents studied containing *c.a.* 10% (w/w) of epoxide was placed in a reaction vial. The same volume of water than organic solvent was added to each vial. The vial were closed and magnetically stirred at 130 ºC for 16 h, and subsequently an aliquot was collected and concentrated under $N_2$. $^1$H NMR revealed that the epoxide group (2.90 ppm, m, **H**COC**H**) was still present in the α-limonene and hexane solutions while it was not observed in the acetone, ethyl acetate and *t*-BuOH solutions. In addition, estolides appeared to be considerable in α-limonene, hexane and ethyl acetate, as determined by the presence of two signals at 3.58 ppm and 4.83 ppm, which can be assigned to **H**-COH (hydrogen bonded to a secondary alcohol) and $R_1COOC\mathbf{H}R_2$ (hydrogen bonded to a secondary alcoxyester), respectively [17]. With respect to acetone and *t*-BuOH, the former presented a partial conversion of the diol moiety into an acetal (3.55 ppm, m, **H**COCO**H**) [40]

whereas the latter presented the best selectivity towards diol moiety formation (3.40 ppm, m, **H**-COH) [4].

In order to achieve a straightforward process to produce DHSA, we expected an optimal amount of *t*-BuOH to allow the epoxide extraction, hydrolysis with hot water and also crystallization of the diol once the reaction had finished. In addition, although *t*-BuOH is not a suitable crystallization solvent due to its high melting point (~25 ºC), the azeotropic mixture with water lowers the melting point, thereby allowing the crystallizations in the fridge (4 ºC). It must be remarked that complete epoxide hydrolysis using an open reactor equipped with a reflux condenser required at least 48 h (results not shown), while 12 h were sufficient to open the epoxide using pressurized reaction vials at 130 ºC. By combining chemo-enzymatic epoxidation, hydrolysis with hot water, and crystallization on the same reaction solvent, we achieved a DHSA yield of 55%. Certainly, this novel process allows an easier preparation of DHSA from oleic acid at lab scale compared to common syntheses using formic acid [23] or methyltrioxorhenium as catalysts [18].

### *3.2. Study of the reactions applied to non-edible animal fat*

#### *3.2.1. Preparation of DHSA from non-edible animal fat*

The highly unsaturated fatty acid mixture from hydrolyzed non-edible animal fat was epoxied, maintaining the double bonds: hydrogen peroxide (1:1.5) ratio used in the oleic acid epoxidation. The crude epoxide yielded crude DHSA using the hot water-*t*-BuOH approach. However, poor yields (~25%) were achieved by direct crystallization of DHSA in *t*-BuOH, probably due to the low percentage of oleic acid in the starting unsaturated mixture (55.14%). Consequently, *t*-BuOH was evaporated and the organic residue was recrystallized from ethyl acetate to increase the

DHSA yield (51%). This DHSA had the same $^{1}$H NMR and melting point as that prepared from commercial oleic acid. Hence, the DHSA prepared from non-edible animal fat was used as the starting material for the syntheses of DHSEs.

*3.2.2. Syntheses of DHSEs from DHSA using a biocatalyst and the corresponding alcohol*

**Figure 4** shows the yields achieved in five consecutive cycles of esterification of DHSA with 1-octanol catalyzed by immobilized CAL-B or *R. oryzae* resting cells using the same amount of biocatalyst. The final yields achieved for the synthesis of pure octyl DHSE using both biocatalysts were nearly 60% during the first four cycles and decreased to 50% on the fifth. *R. oryzae* resting cells achieved slightly lower yields in most of the cycles. However, the catalytic performance of the two biocatalysts was similar. Indeed, 0.1 g of immobilized CAL-B or *R. oryzae* cells yielded 4.75 g and 4.56 g of pure octyl DHSE, respectively.

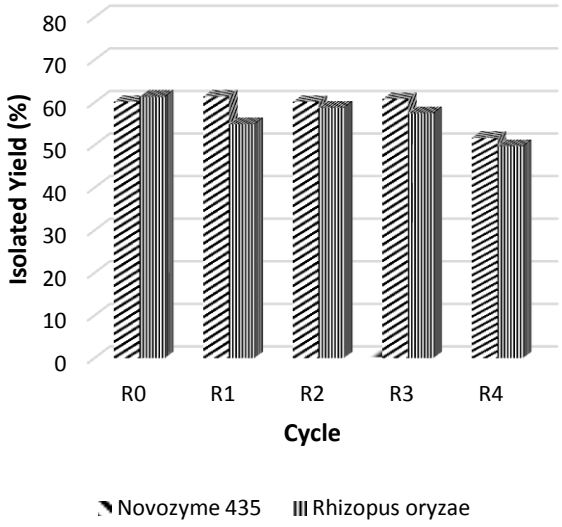


**Figure 4**. Isolated yield for the esterification of 1-octanol with DHSA catalyzed by immobilized CAL-B or *R. oryzae* resting cells at 40º C for 24 h in α-limonene. Data correspond to five experimental cycles using the same recovered biocatalyst.

Finally, immobilized CAL-B was used as a biocatalyst to prepare various DHSEs. An alcohol excess ranging 5:1 to 1.1:1 was studied (results not shown). **Table 1** shows the best alcohol:DHSA ratio for the preparation of each ester. The crystallization temperatures and the yields achieved are also showed. To the best of our knowledge, this is the first study to report the yields of crystallized DHSEs prepared by enzymatic esterification from DHSA using α-limonene as solvent. In the present study, the use of α-limonene and a suitable crystallization temperature allowed the recovery of the esters without solvent evaporation, which represents an important energy saving. In addition, most of the yields achieved were higher than those reported by Swern et al. [38] using naphthalene-β-sulfonic acid as catalyst and higher amounts of alcohol at 100ºC.

*3.3. Thermal properties and cycling reliability of the DHSEs from non-edible animal fat*

**Table 2** shows the thermal properties of the twelve DHSEs prepared. The melting temperatures of these esters ranged from 52.45 ºC to 76.88 ºC and the solidification temperatures from 40.04 ºC to 70.82 ºC. These phase-change temperatures meet the requirements of the following equipment: domestic hot water (DHW) tanks [41,42], air conditioning condensation heat recovery systems [7], and low temperature industrial waste heat (IWH) recovery in industries such as those devoted to food and beverage, textile, paper, and non-metallic mineral processes [43]. However, sub-cooling ranging from 17.15 ºC to 7.20 ºC was observed in the DSC analysis. This effect may be related to the DSC analysis method [44]. Nevertheless, the diol moiety of these DHSEs could account for such sub-cooling since the DSC analysis of some polyols, such as erythritol [45] and galactitol [46], also revealed this effect. DSC curves of the bio-based mixtures prepared from non-edible fats showed a sharp endothermic peak during melting and a sharp exothermic peak during solidification, thereby indicating that a pure product was obtained at the end of the synthetic process (see **SI**). The non-cycled melting latent heats of the esters prepared ranged from 136.83 $kJ \bullet kg^{-1}$ to 234.22 $kJ \bullet kg^{-1}$ and latent heat of solidification from 122.68 $kJ \bullet kg^{-1}$ to 229.71 $kJ \bullet kg^{-1}$. Thus, some of these DHSEs showed enthalpy values comparable to paraffin, which has a latent heat of solidification in the range of 180 $kJ \bullet kg^{-1}$ to 230 $kJ \bullet kg^{-1}$ [9]. These DHSEs showed some similarities when compared to analogous stearates studied for PCM purposes. As an example, odd carbon-numbered alcohol esters such as methyl and propyl stearates presented higher latent heats than even carbon-numbered esters such as ethyl and butyl stearates [28,47]. However, the melting temperatures of these four alcoxyl stearates were nearly 30 ºC lower than their DHSE counterparts. Indeed, to prepare stearates as

PCMs with melting temperatures of around 60 ºC, high-chain esters such as octadecyl stearate (59.22 ºC) are required [29].

**Table 2.** Thermal properties of the DHSEs prepared from non-edible animal fat (see **SI**).

| Alkyl DHSE | $H_{melting}$ (kJ•kg$^{-1}$) | $H_{solidification}$ (kJ•kg$^{-1}$) | $T_{melting}$ (ºC) | $T_{solidification}$ (ºC) |
|---|---|---|---|---|
| Methyl | 181.40±0.08 | 156.26±0.83 | 69.31±0.00 | 53.86±0.37 |
| Ethyl | 142.29±1.65 | 140.70±0.01 | 57.06±0.01 | 47.50±0.09 |
| Propyl | 148.82±2.52 | 138.03±1.71 | 58.75±0.01 | 43.25±0.42 |
| Butyl | 136.83±1.88 | 122.68±2.62 | 52.45±0.01 | 40.04±0.00 |
| Pentyl | 155.54±1.90 | 145.01±2.04 | 55.34±0.14 | 42.51±0.63 |
| Hexyl | 213.30±0.30 | 201.91±0.54 | 63.93±0.05 | 48.37±0.23 |
| Octyl | 234.22±3.47 | 229.71±3.13 | 72.65±0.04 | 64.57±0.15 |
| Decyl | 216.62±0.55 | 203.31±2.15 | 72.27±0.01 | 55.12±0.28 |
| Dodecyl | 215.41±2.87 | 200.31±2.80 | 70.70±0.02 | 55.63±0.98 |
| Tetradecyl | 191.74±1.26 | 147.27±0.91 | 71.12±0.01 | 60.60±0.01 |
| Hexadecyl | 178.77±2.75 | 175.45±5.99 | 71.61±0.01 | 64.41±0.23 |
| Octadecyl | 160.83±11.29 | 168.50±6.43 | 76.88±0.06 | 70.82±0.08 |

On the other hand, some of the described commercial fatty acid bio-based PCMs [11,12,14] and the bio-based eutectic mixture from non-edible animal fat prepared by some of the authors [4] presented latent heats of solidification ranging 150 kJ•kg$^{-1}$ [11,12,14] to 180 kJ•kg$^{-1}$ [4]. Certainly, some of the DHSEs prepared in the present study shown higher enthalpies. For that reason, the cycling reliability of the products showing enthalpies above 200 kJ•kg$^{-1}$ was studied. Thermal cycling tests are essential to ensure the applicability of a PCM since its working principle relies on repeated melting and freezing cycles. The purpose of such tests is to ensure

that the thermo-physical properties of a PCM remain constant or do not show a variation of more than ± 20% compared to their initial value after cycling [48].

The variation of solidification and melting enthalpies after 100 thermal cycles ranged from a gain of 0.99% to a loss of 2.94% (see **Table 3**). Losses below 20% after thermal cycling indicate that the material shows good thermal cycling stability [49]. Moreover, octyl DHSE showed the highest latent heat after 100 heating/cooling cycles: 230.05 $kJ \cdot kg^{-1}$ (fusion enthalpy), 228.69 $kJ \cdot kg^{-1}$ (solidification enthalpy). In addition, only the phase-change solidification temperature of hexyl DHSE presented outstanding changes (13.34%). Given these findings, thermal cycling stability tests were taken one step further, and 1000 thermal cycles were performed following the same methodology.

The results from the 1000 thermal cycles (**Table 3**) reveal that solidification and melting enthalpies varied from a gain of 5.36 % to a loss of 11.78 %. On the one hand, dodecyl DHSE showed the most significant reduction in thermal performance with an 11.78 % loss of melting enthalpy. On the other hand, octyl DHSE again showed the highest melting and solidification enthalpies after 1000 heating/cooling cycles (223 $kJ \cdot kg^{-1}$ and 218 $kJ \cdot kg^{-1}$, respectively). Of the distinct esters prepared, hexyl DHSE presented the best thermal cycling stability since melting and solidification enthalpies did not decreases more than 4% after thermal cycling stability tests.

**Table 3.** Thermal cycling stability results of DHSEs with high thermal storage capacity (see **SI**).

| Alkyl DHSE | Reliability | $H_{melting}$ ($kJ \cdot kg^{-1}$) | $H_{solidification}$ ($kJ \cdot kg^{-1}$) | $T_{melting}$ ($^oC$) | $T_{solidification}$ ($^oC$) |
|---|---|---|---|---|---|
| Hexyl | Cycled 100 | 213.55±6.25 | 200.46±4.38 | 63.99±0.03 | 41.92±0.08 |
| | Property loss (%) | -0.12 | 0.72 | -0.10 | 13.34 |
| | Cycled 1000 | 212.84±0.78 | 194.33±5.13 | 64.03±0.04 | 40.98±1.22 |
| | Property loss (%) | 0.21 | 3.75 | -0.16 | 15.28 |
| Octyl | Cycled 100 | 230.05±0.06 | 228.69±1.04 | 72.78±0.04 | 64.65±0.02 |
| | Property loss (%) | 1.78 | 0.44 | -0.18 | -0.12 |
| | Cycled 1000 | 221.61±4.59 | 217.82±12.60 | 72.55±0.23 | 60.45±4.14 |
| | Property loss (%) | 5.38 | 5.17 | 0.14 | 6.37 |
| Decyl | Cycled 100 | 218.78±2.55 | 209.22±2.41 | 72.52±0.02 | 57.07±0.08 |
| | Property loss (%) | -0.99 | -2.90 | -0.35 | -3.54 |
| | Cycled 1000 | 217.52±6.06 | 214.22±1.00 | 72.33±0.01 | 58.25±2.68 |
| | Property loss (%) | -0.41 | -5.36 | -0.09 | -5.67 |
| Dodecyl | Cycled 100 | 209.26±2.35 | 200.87±2.81 | 70.74±0.06 | 55.52±0.23 |
| | Property loss (%) | 2.86 | -0.28 | -0.06 | 0.21 |
| | Cycled 1000 | 190.03±3.25 | 194.74±4.04 | 70.06±0.16 | 56.34±0.21 |
| | Property loss (%) | 11.78 | 2.78 | 0.90 | -1.27 |

From the phase-change temperature point of view, none of the materials tested experienced a temperature change of more than 16%. Nevertheless, the results suggest that thermal cycling

increases the sub-cooling effect in several materials. For example, the solidification temperature of hexyl DHSE and octyl DHSE decreased from 48 ºC to 40 ºC and from 65 ºC to 60 ºC, respectively. The principal drawback of these materials as PCMs is their sub-cooling, which was increased in some cases by thermal cycling, at least at lab scale. However, some PCMs showed no sub-cooling or less sub-cooling when tested at higher scales, such as hundreds of kilograms, amounts closer to real applications [50].

On the basis of the thermal properties experimentally obtained and thermal cycling tests results, the preparation of DHSEs improved the thermal stability of DHSA and expanded the application scope. Besides, the diol moiety could easily be modified to groups such as ketals [40] or acetals [21,40] with substantial lower melting points. In the case of showing good thermal properties these compounds should boost the potential scope of fatty acid bio-based PCM.

## 4. Conclusion

Non-edible animal fat was converted successfully into DHSEs that showed good thermal properties as PCMs. These DHSEs were synthesized using biocatalysts. Final products were purified by direct crystallization on the reaction solvent. Biocatalyst reusability in the epoxidation step was studied in terms of productivity using a model compound (commercial oleic acid). Besides, immobilized CAL-B successfully afforded the enzymatic final esterification during various cycles. In addition, *R. oryzae* resting cells showed a similar performance in this esterification process. α-Limonene showed a high capacity to preserve biocatalyst activity and allowed the preparation of twelve DHSEs by crystallization. The preparation and thermal analysis of these esters is a step forward. The products synthesized extend the applications of non-edible fats as feedstock to prepare these esters (as bio-PCM) showing high enthalpies (up to

234 kJ•kg$^{-1}$), attractive range of operation (52.45 ºC to 76.88 ºC) and also good thermal stability after 1000 cycles.

**Acknowledgments**

GREA and DBA are certified agents TECNIO in the category of technology developers from the Government of Catalonia. We thanks to Subproductos Cárnicos Echevarria y Asociados S.L (Cervera, Spain) for supplying the non-edible fat.

Moreover, the research leading to these results has received funding from the European Commission Seventh Framework Programme (FP/2007-2013) under grant agreement n° PIRSES-GA-2013-610692 (INNOSTORAGE) and from the European Union's Horizon 2020 research and innovation program under grant agreement n° 657466 (INPATH-TES). The authors would like to thank the Catalan Government for the quality accreditation given to their research groups GREA (2014 SGR 123) and Agricultural Biotechnology Research Group (2014 SGR 1296). This work has been partially funded by the Spanish government (CTQ2015-70982-C3-1-R (MINECO/FEDER) and ENE2015-64117-C5-1-R (MINECO/FEDER). Aran Solé would like to thank Ministerio de Economía y Competitividad de España for Grant Juan de la Cierva, FJCI-2015-25741.

**References**

[1] J. Bongaarts, Human population growth and the demographic transition. Philos. Trans. R. Soc. B, Biol. Sci. 364 (2009) 2985–2990.

[2] A. Irshad, S. Sureshkumar, A. Shalima Shukoor, M. Sutha, Slaughter house by-product utilization for sustainable meat industry- a review. IJDR 6 (2015) 4725-4734.

[3] C. Öner, Ş. Altun, Biodiesel production from inedible animal tallow and an experimental investigation of its use as alternative fuel in a direct injection diesel engine. Appl. Energy 86 (2009) 2114–2120.

[4] P. Gallart-Sirvent, M. Martín, G. Villorbina, M. Balcells, A. Solé, C. Barrenche, L. F. Cabeza, R. Canela-garayoa, Fatty acids and derivatives from non-edible animal fat as phase change materials. RSC Adv. 7 (2017) 24133-24139.

[5] Y. Yuan, N. Zhang, W. Tao, X. Cao, Y. He, Fatty acids as phase change materials: A review. Renew. Sustain. Energy Rev. 29 (2014) 482–498.

[6] B. Zalba, J. M. Marín, L. F. Cabeza, H. Mehling, Review on thermal energy storage with phase change: Materials, heat transfer analysis and applications. Appl. Therm. Eng. 23 (2003) 251-283.

[7] N. Zhang, Y. Yuan, Y. Du, X. Cao, Y. Yuan, Preparation and properties of palmitic-stearic acid eutectic mixture/expanded graphite composite as phase change material for energy storage. Energy 78 (2014) 950–956.

[8] M. M. Farid, A. M. Khudhair, S. A. K. Razack, S. Al-Hallaj, A review on phase change energy storage: Materials and applications. Energy Convers. Manag. 45 (2004) 1597–1615.

[9] W. Hu, X. Yu, Thermal and mechanical properties of bio-based PCMs encapsulated with nanofibrous structure. Renew. Energy 62 (2014) 454–458.

[10] W. Hu, X. Yu, Encapsulation of bio-based PCM with coaxial electrospun ultrafine fibers.

RSC Adv. 2 (2012) 5580–5584.

[11] S. Yu, S.G. Jeong, O. Chung, S. Kim, Bio-based PCM/carbon nanomaterials composites with enhanced thermal conductivity. Sol. Energy Mater. Sol. Cells 120 (2014) 549–554.

[12] S.G. Jeong, O. Chung, S. Yu, S. Kim, S. Kim, Improvement of the thermal properties of Bio-based PCM using exfoliated graphite nanoplatelets. Sol. Energy Mater. Sol. Cells 117 (2013) 87–92.

[13] J. Kosny, E. Kossecka, A. Brzezinski, A. Tleoubaev, D. Yarbrough, Dynamic thermal performance analysis of fiber insulations containing bio-based phase change materials (PCMs). Energy Build. 52 (2012) 122–131.

[14] S. G. Jeong, J. H. Lee, J. Seo, S. Kim, Thermal performance evaluation of Bio-based shape stabilized PCM with boron nitride for energy saving. Int. J. Heat Mass Transf. 71 (2014) 245–250.

[15] A.E. Atabani, A.S. Silitonga, H. C. Ong, T. M. I. Mahlia, H. H. Masjuki, I. A. Badruddin, H. Fayaz, Non-edible vegetable oils: A critical evaluation of oil extraction, fatty acid compositions, biodiesel production, characteristics, engine performance and emissions production. Renew. Sustain. Energy Rev. 18 (2013) 211–245.

[16] A. Li, K. Li, Pressure-sensitive adhesives based on epoxidized soybean oil and dicarboxylic acids. ACS Sustain. Chem. Eng. 2 (2014) 2090–2096.

[17] Y. Wu, A. Li, K. Li, Pressure Sensitive Adhesives based on oleic acid. J. Am. Oil Chem. Soc. 92 (2014) 111–120.

[18] M. A. R. Meier, J. O. Metzger, U. S. Schubert, Plant oil renewable resources as green alternatives in polymer science. Chem. Soc. Rev. 36 (2007) 1788–1802.

[19] A. Kulik, A. Martin, M. M. Pohl, C. Fischer, A. Köckritz, Insights into gold-catalyzed synthesis of azelaic acid. Green Chem. 16 (2014) 1799-1806.

[20] A. Kulik, A. Janz, M. M. Pohl, A. Martin, A. Köckritz, Gold-catalyzed synthesis of dicarboxylic and monocarboxylic acids. Eur. J. Lipid Sci. Technol. 114 (2012) 1327–1332.

[21] J. Filley, New lubricants from vegetable oil: Cyclic acetals of methyl 9,10-dihydroxystearate. Bioresour. Technol. 96 (2005) 551–555.

[22] G. F. L. Koay, T. Chuah, S. Zainal-Abidin, S. Ahmad, T. S. Y. Choong, Development, characterization and commercial application of palm based dihydroxystearic acid and its derivatives: an overview. J. Oleo. Sci. 265 (2011) 237–265.

[23] D. Swern, J.T. Scanlan, G. B. Dickel, 9,10-Dihydroxystearic acid. Org. Synth. 39 (1959) 15.

[24] S. Ahmad, R. Awang, H. Abu Hassan, M. Norhisham Sattar, H. Seng Soi, Y. Amiyati Yusof, Palm oil-based hydroxy fatty acids. EP001588999A2. 2005.

[25] D.L. Gaveau, S. Wich, J. Epting, D. Juhn, M. Kanninen, N. Leader-Williams, The future of forests and orangutans (Pongo abelii) in Sumatra: predicting impacts of oil palm plantations, road construction, and mechanisms for reducing carbon emissions from deforestation. Environ. Res. Lett. 4 (2009) 34013-34024.

[26] E.B. Fitzherbert, M. J. Struebig, A. Morel, F. Danielsen, C. A. Brühl, P. F. Donald, B. Phalan, How will oil palm expansion affect biodiversity? Trends Ecol. Evol. 23 (2008) 538–545.

[27] L. P. Koh, D. S. Wilcove, Is oil palm agriculture really destroying tropical biodiversity? Conserv. Lett. 1 (2008) 60–64.

[28] G. F. Suppes, M. J. Goff, S. Lopes, Latent heat characteristics of fatty acid derivatives pursuant phase change material applications. Chem. Eng. Sci. 58 (2003) 1751–1763.

[29] A. Alper Aydn, High-chain fatty acid esters of 1-octadecanol as novel organic phase change materials and mathematical correlations for estimating the thermal properties of higher fatty acid esters' homologous series. Sol. Energy Mater. Sol. Cells 113 (2013) 44–51.

[30] A. A. Aydın, A. Aydın, High-chain fatty acid esters of 1-hexadecanol for low temperature thermal energy storage with phase change materials. Sol. Energy Mater. Sol. Cells 96 (2012) 93–100.

[31] A. A. Aydn, H. Okutan, High-chain fatty acid esters of myristyl alcohol with odd carbon number: Novel organic phase change materials for thermal energy storage - 1. Sol. Energy Mater. Sol. Cells 95 (2011) 2752–2762.

[32] A. A. Aydn, H. Okutan, High-chain fatty acid esters of myristyl alcohol with odd carbon number: Novel organic phase change materials for thermal energy storage - 2. Sol. Energy Mater. Sol. Cells 95 (2011) 2417–2423.

[33] L. Raghunanan, M. C. Floros, S. S. Narine, Thermal stability of renewable diesters as phase change materials. Thermochim. Acta 644 (2016) 61–68.

[34] R. Awang, M. Basri, S. Ahmad, A. B. Salleh, Enzymatic esterification of dihydroxystearic acid. J. Am. Oil Chem. Soc. 77 (2000) 609–612.

[35] R. Awang, M. Basri, S. Ahmad, A. B. Salleh, Lipase catalyzed esterification of palm based 9, 10-dihydroxystearic acid and 1-octanol in hexane – a kinetic study. Biotechnol. Lett. 6 (2004) 11–14.

[36] P. Gallart-Sirvent, E. Yara, G. Villorbina, M. Balcells, N. Sala, R. Canela-Garayoa, Recycling Rhizopus oryzae resting cells as biocatalyst to prepare near eutectic palmitic-stearic acid mixtures from non-edible fat. J. Mol. Catal. B Enzym. 134 (2016) 172–177.

[37] J. Eras, F. Montañes, J. Ferran, R. Canela, Chlorotrimethylsilane as a reagent for gas chromatographic analysis of fats and oils. J. Chromatogr. A 918 (2001) 227–232.

[38] D. Swern, E. F. Jordan, Aliphatic esters of the 9,l0-dihydroxystearic acids. J. Am. Chem. Soc. 67 (1945) 902–903.

[39] D. Prat, A. Wells, J. Hayler, H. Sneddon, C. R. McElroy, S. Abou-Shehada, P. J. Dunn, CHEM21 selection guide of classical- and less classical-solvents. Green Chem. 18 (2016) 288–296.

[40] A. Godard, A. Thiebaud-Roux, P. De Caro, E. Vedrenne, Z. Mouloungui, New one-pot syntheses of ketals and acetals from oleic acid. Ind. Crops Prod. 52 (2014) 111–117.

[41] L. F. Cabeza, A. Castell, C. Barreneche, A. De Gracia, A. I. Fernández, Materials used as

PCM in thermal energy storage in buildings: A review. Renew. Sustain. Energy Rev. 15 (2011) 1675–1695.

[42] T. Kousksou, P. Bruel, G. Cherreau, V. Leoussoff, T. El Rhafiki, PCM storage for solar DHW: From an unfulfilled promise to a real benefit. Sol. Energy 85 (2011) 2033–2040.

[43] S. Brückner, S. Liu, L. Miró, M. Radspieler, L. F. Cabeza, E. Lävemann, Industrial waste heat recovery technologies: An economic analysis of heat transformation technologies. Appl. Energy 151 (2015) 157–167.

[44] E. Günther, S. Hiebler, H. Mehling, R. Redlich, Enthalpy of phase change materials as a function of temperature: Required accuracy and suitable measurement methods. Int. J. Thermophys. 30 (2009) 1257–1269.

[45] A. Sari, R. Eroglu, A. Biçer, A. Karaipekli, Synthesis and thermal energy storage properties of erythritol tetrastearate and erythritol tetrapalmitate. Chem. Eng. Technol. 34 (2011) 87–92.

[46] A. Sari, A. Biçer, Ö. Lafçi, M. Ceylan, Galactitol hexa stearate and galactitol hexa palmitate as novel solid-liquid phase change materials for thermal energy storage. Sol. Energy 85 (2011) 2061–2071.

[47] D. Feldman, D. Banu, D. Hawes, Low chain esters of stearic acid as phase change materials for thermal energy storage in buildings. Sol. Energy Mater. Sol. Cells 36 (1995) 311–322.

[48] A. Solé, H. Neumann, S. Niedermaier, I. Martorell, P. Schossig, L. F. Cabeza, Stability of

sugar alcohols as PCM for thermal energy storage. Sol. Energy Mater. Sol. Cells 126 (2014) 125–134.

[49] A. Solé, H. Neumann, S Niedermaier, L. F. Cabeza, E. Palomo, Thermal stability test of sugar alcohols as phase change materials for medium temperature energy storage application. Energy Procedia 48 (2014) 436–439.

[50] A. Gil, C. Barreneche, P. Moreno, C. Solé, A. Inés Fernández, L. F. Cabeza, Thermal behaviour of d-mannitol when used as PCM: Comparison of results obtained by DSC and in a thermal energy storage unit at pilot plant scale. Appl. Energy 111 (2013) 1107–1113.

# Combining biocatalysts to achieve new phase change materials. Application to non-edible animal fat

*Pau Gallart-Sirvent*[a], *Marc Martín*[b], *Aran Solé* [c], *Gemma Villorbina*[a], *Mercè Balcells*[a], *Luisa F. Cabeza**[,b], *Ramon Canela-Garayoa*[*,a]

[a] Department of Chemistry-DBA center, University of Lleida, ETSEA, Av. Rovira Roure 191, 25198, Lleida, Spain

[b] GREA Innovació concurrent, INSPIRES Research Centre, University of Lleida, Pere de Cabrera s/n, 25001, Lleida, Spain

[c] Department of Mechanical Engineering and Construction, Universitat Jaume I, Campus del Riu Sec s/n, 12071 Castelló de la Plana, Spain

*Corresponding authors:

canela@quimica.udl.cat and lcabeza@diei.udl.cat

**SUMMARY:**

**DSC analysis of the DHSEs**

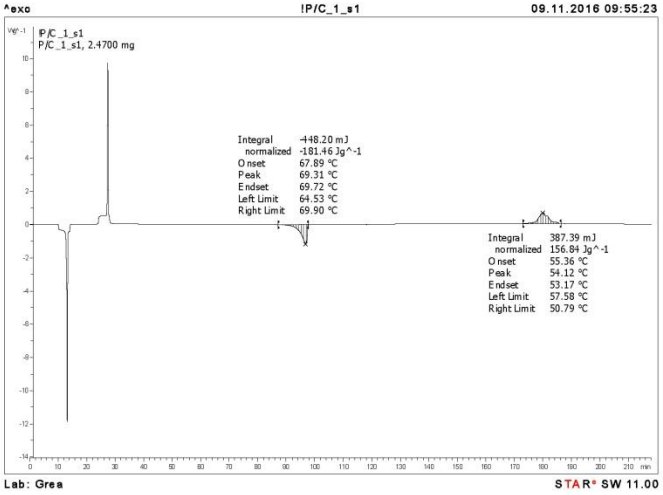


**Figure 1.** DSC response and evaluation of methyl DHSE. Not cycled sample 1.

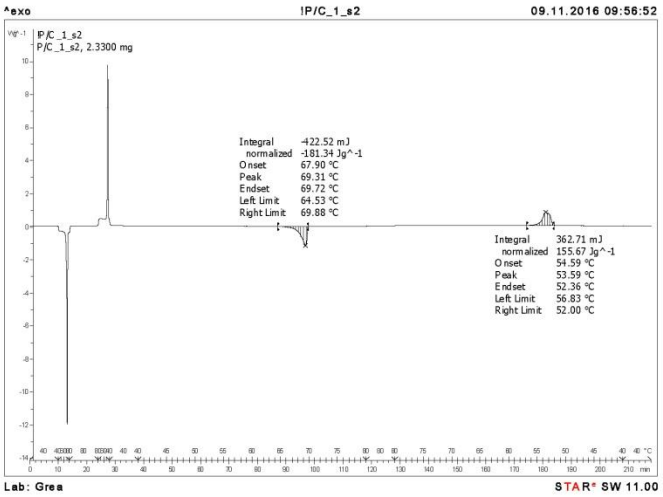


**Figure 2.** DSC response and evaluation of methyl DHSE. Not cycled sample 2.

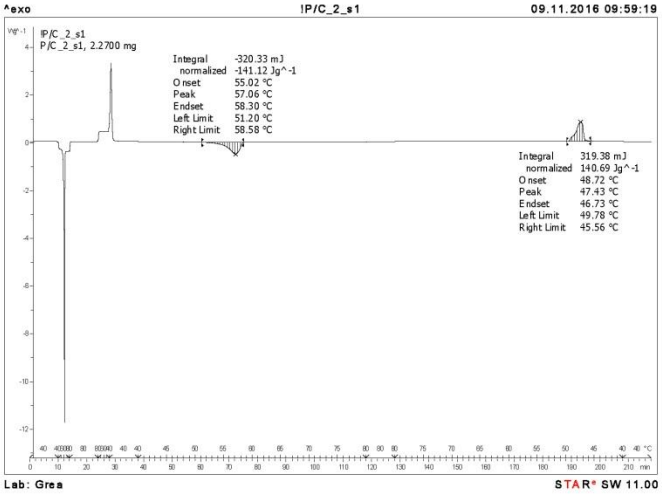


**Figure 3.** DSC response and evaluation of ethyl DHSE. Not cycled sample 1.

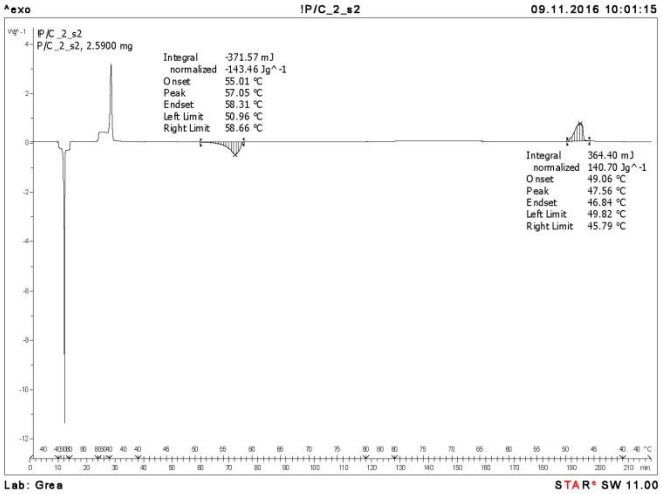


**Figure 4.** DSC response and evaluation of ethyl DHSE. Not cycled sample 2.

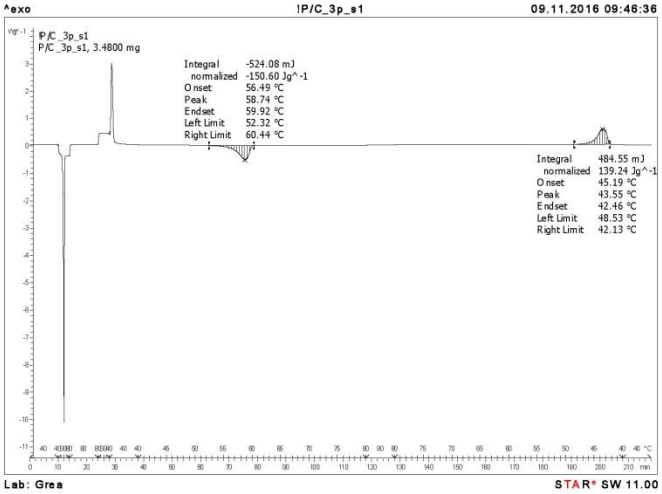


**Figure 5.** DSC response and evaluation of propyl DHSE. Not cycled sample 1.

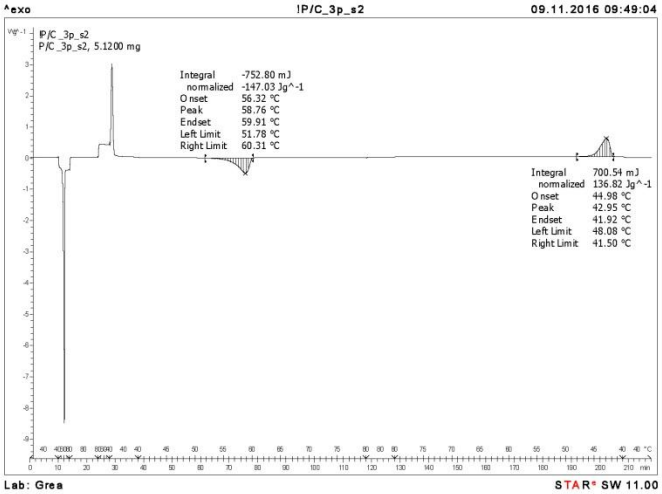


**Figure 6.** DSC response and evaluation of propyl DHSE. Not cycled sample 2.

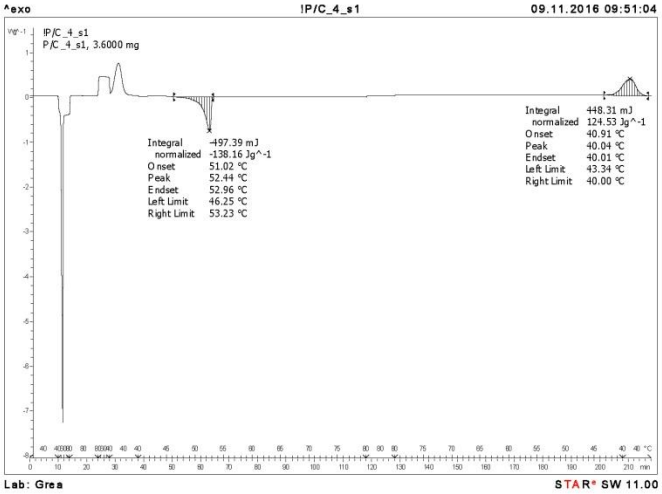


**Figure 7.** DSC response and evaluation of butyl DHSE. Not cycled sample 1.

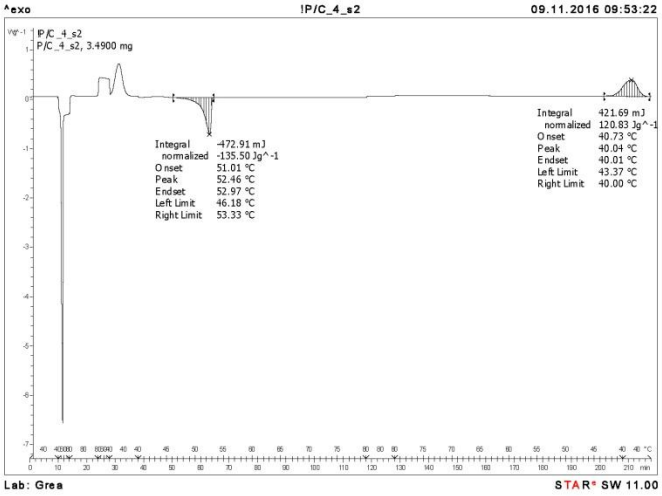


**Figure 8.** DSC response and evaluation of butyl DHSE. Not cycled sample 2.

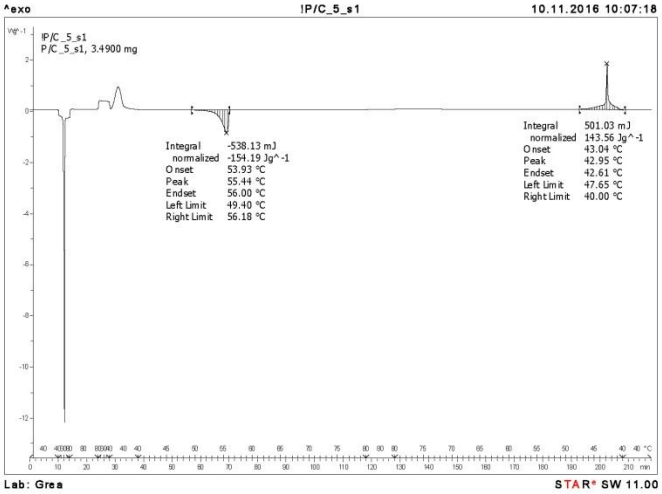


**Figure 9.** DSC response and evaluation of pentyl DHSE. Not cycled sample 1.

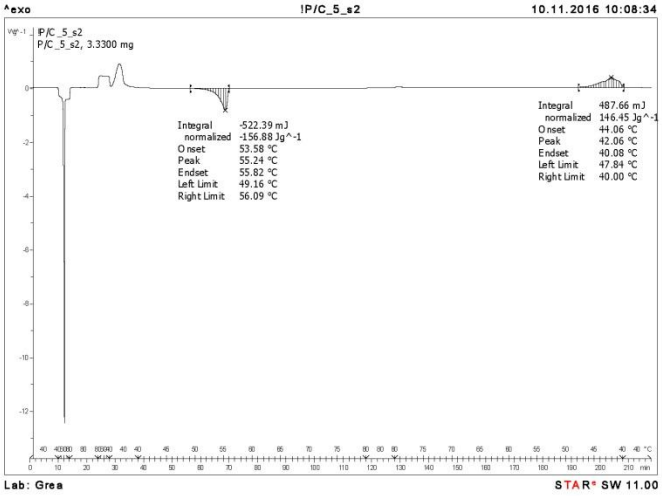


**Figure 10.** DSC response and evaluation of pentyl DHSE. Not cycled sample 2.

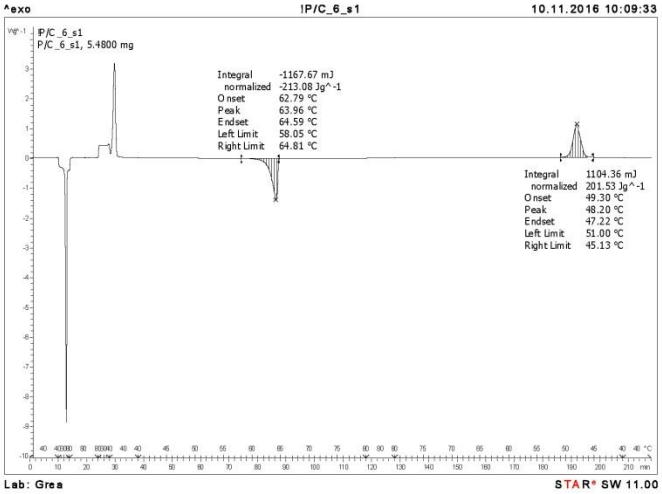


**Figure 11.** DSC response and evaluation of hexyl DHSE. Not cycled sample 1.

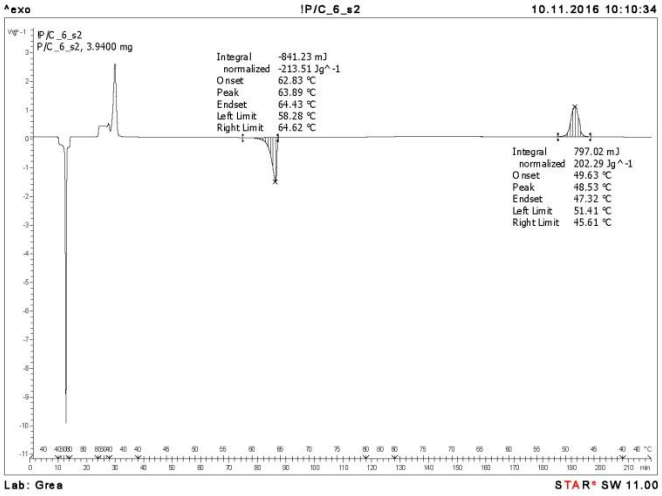


**Figure 12.** DSC response and evaluation of hexyl DHSE. Not cycled sample 2.

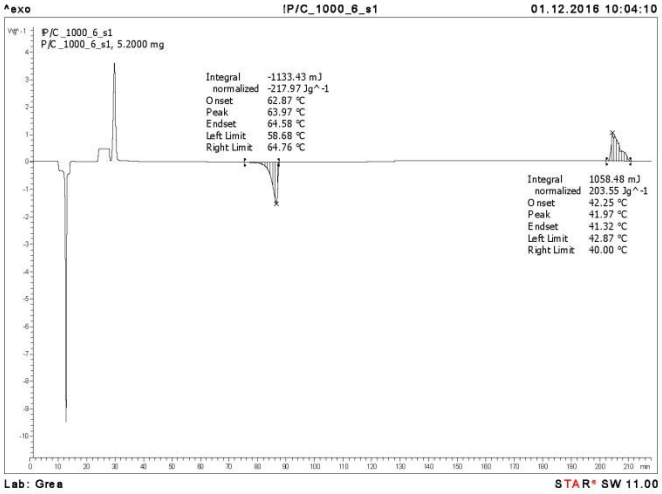


**Figure 13.** DSC response and evaluation of hexyl DHSE. Cycled sample 1. 100 cycles.

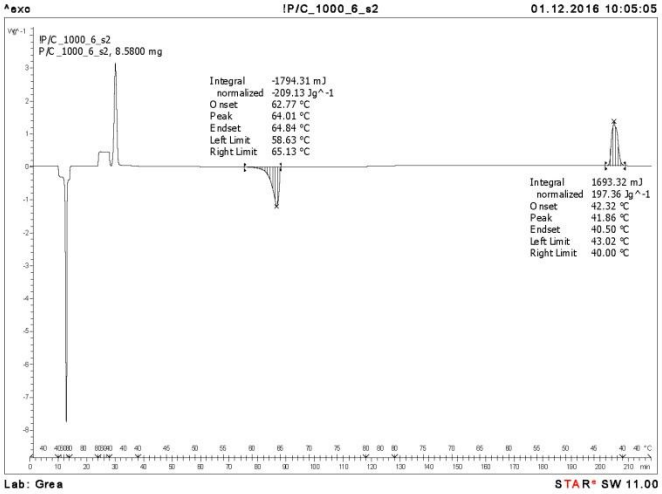


**Figure 14.** DSC response and evaluation of hexyl DHSE. Cycled sample 2. 100 cycles.

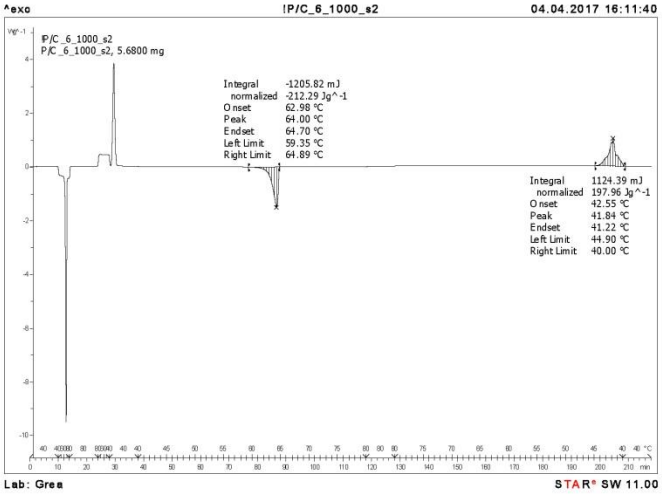


**Figure 15.** DSC response and evaluation of hexyl DHSE. Cycled sample 1. 1000 cycles.

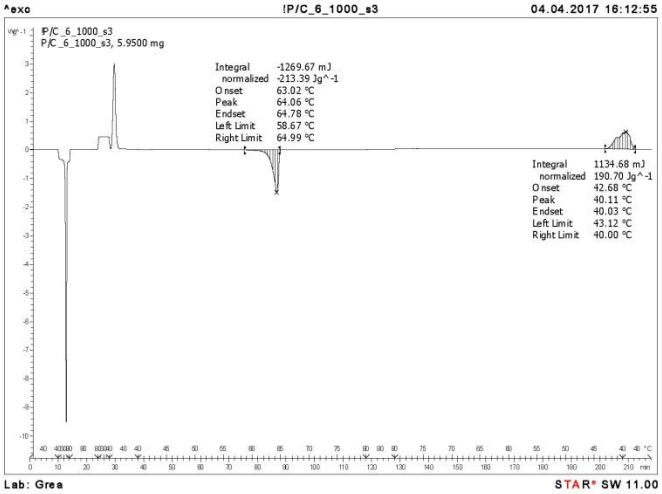


**Figure 16.** DSC response and evaluation of hexyl DHSE. Cycled sample 2. 1000 cycles.

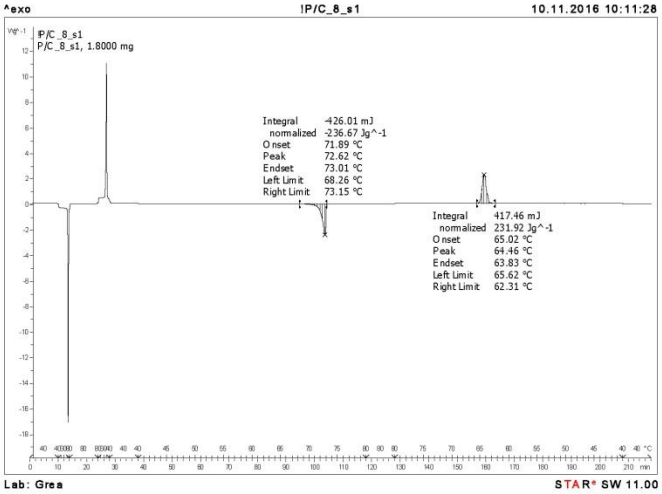


**Figure 17.** DSC response and evaluation of octyl DHSE. Not cycled sample 1.

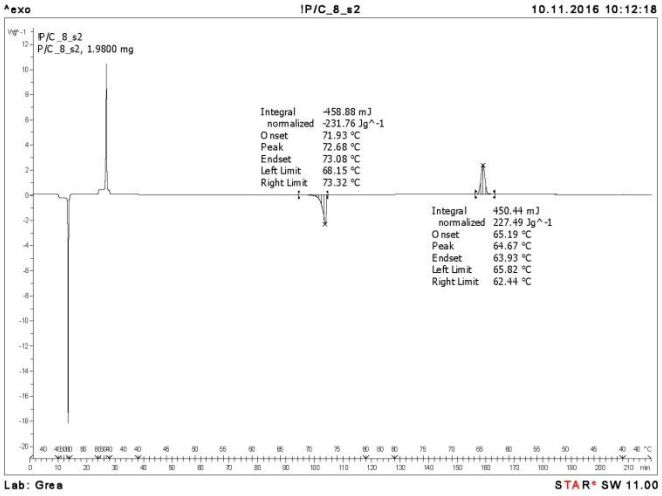


**Figure 18.** DSC response and evaluation of octyl DHSE. Not cycled sample 2.

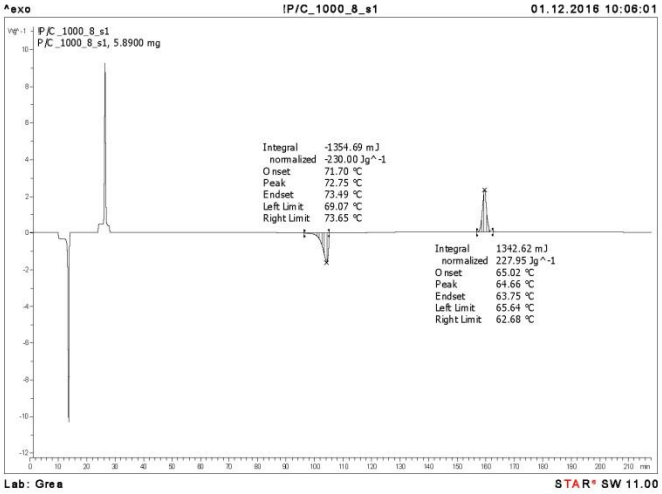


**Figure 19.** DSC response and evaluation of octyl DHSE. Cycled sample 1. 100 cycles.

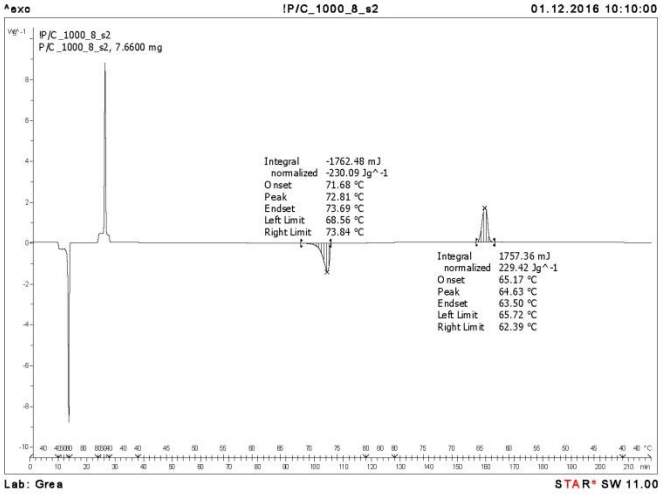


**Figure 20.** DSC response and evaluation of octyl DHSE. Cycled sample 2. 100 cycles.

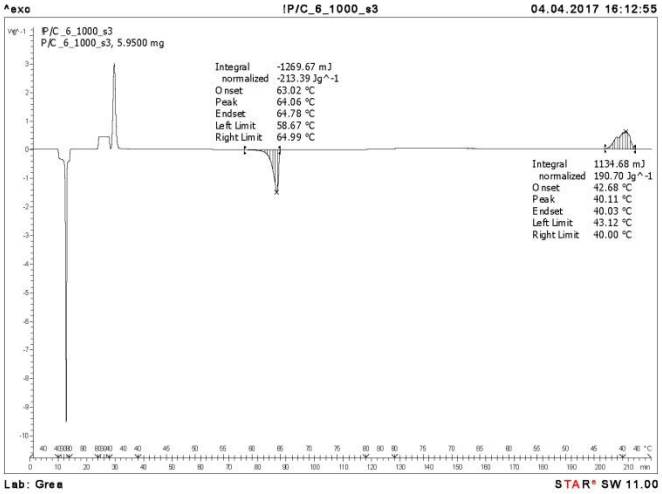


**Figure 21.** DSC response and evaluation of octyl DHSE. Cycled sample 1. 1000 cycles.

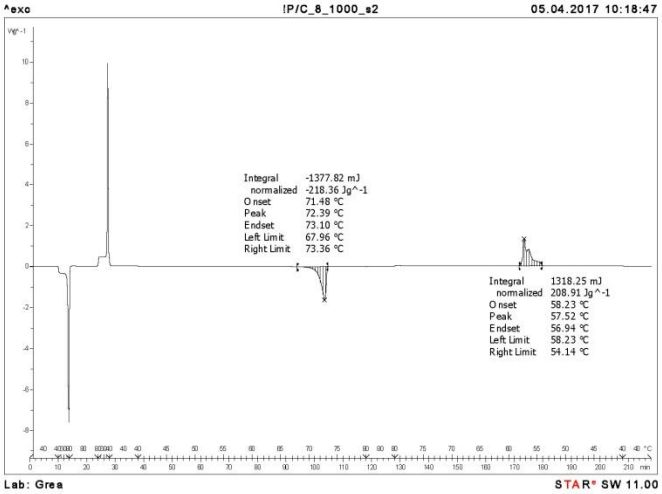


**Figure 22.** DSC response and evaluation of octyl DHSE. Cycled sample 2. 1000 cycles.

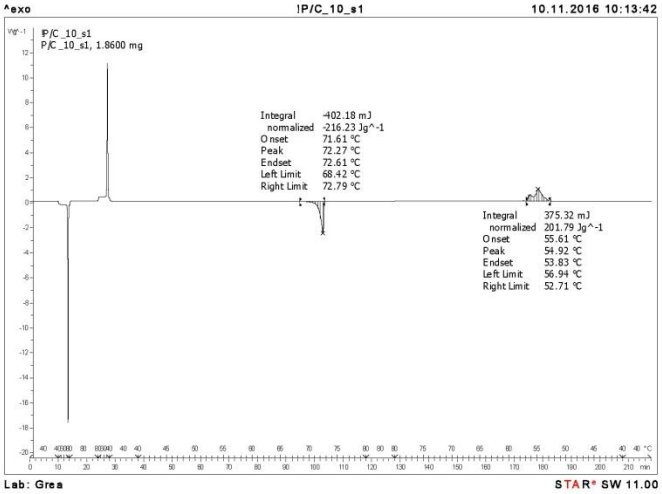


**Figure 23.** DSC response and evaluation of decyl DHSE. Not cycled sample 1.

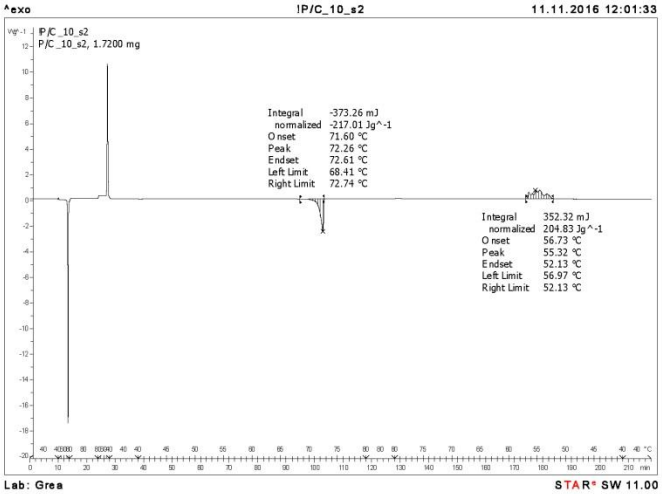


**Figure 24.** DSC response and evaluation of decyl DHSE. Not cycled sample 2.

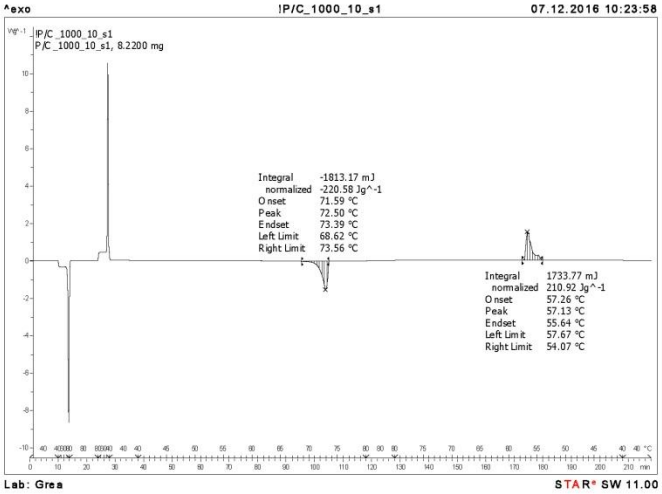


**Figure 25.** DSC response and evaluation of decyl DHSE. Cycled sample 1. 100 cycles.

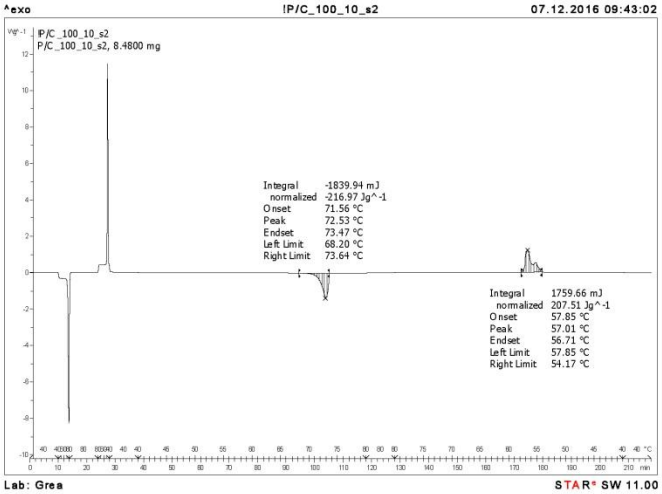


**Figure 26.** DSC response and evaluation of decyl DHSE. Cycled sample 2. 100 cycles.

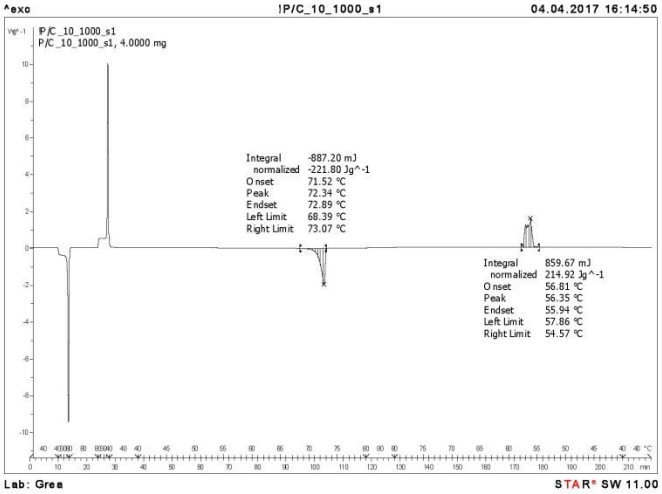


**Figure 27.** DSC response and evaluation of decyl DHSE. Cycled sample 1. 1000 cycles.

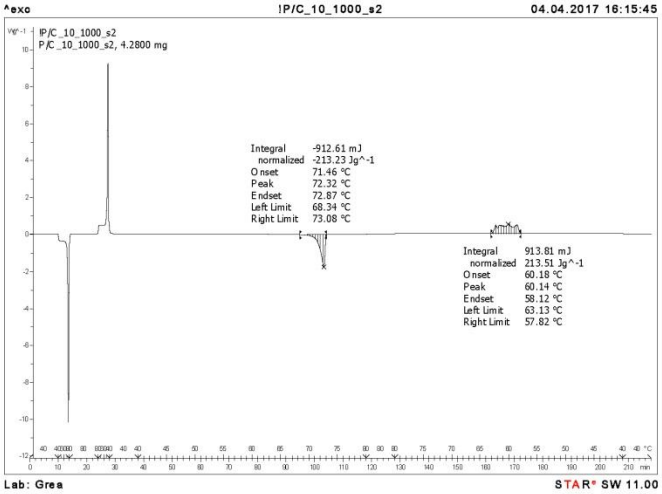


**Figure 28.** DSC response and evaluation of decyl DHSE. Cycled sample 2. 1000 cycles.

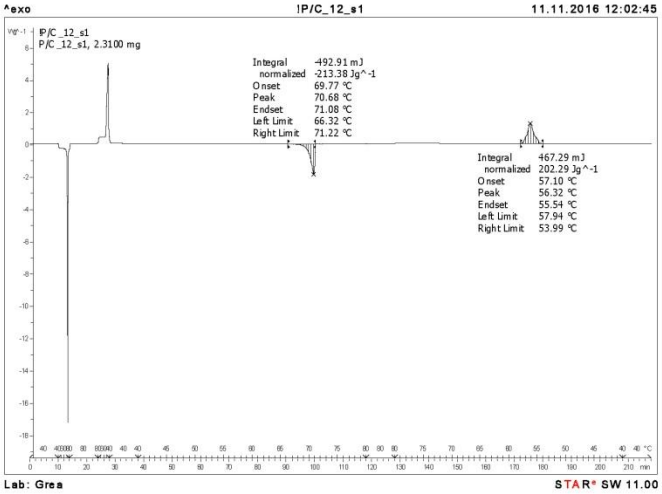


**Figure 29.** DSC response and evaluation of dodecyl DHSE. Not cycled sample 1.

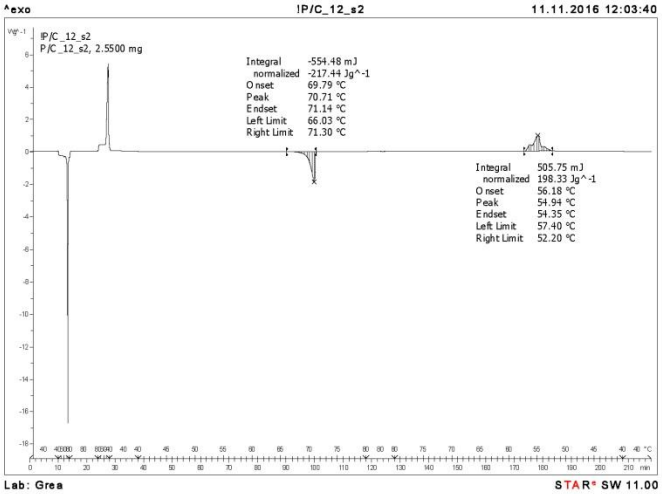


**Figure 30.** DSC response and evaluation of dodecyl DHSE. Not cycled sample 2.

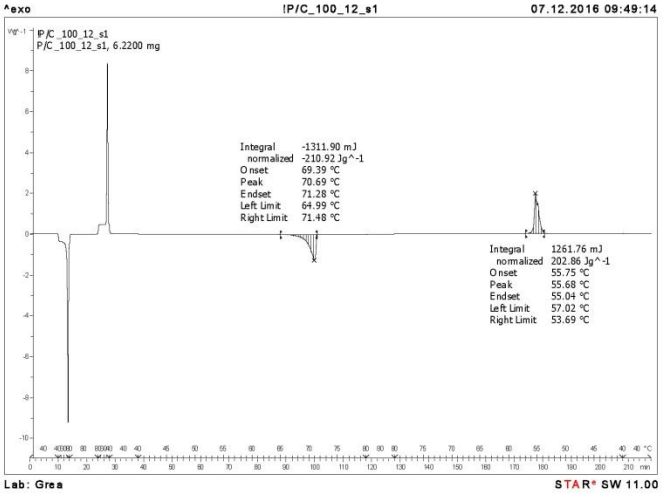


**Figure 31.** DSC response and evaluation of dodecyl DHSE. Cycled sample 1. 100 cycles.

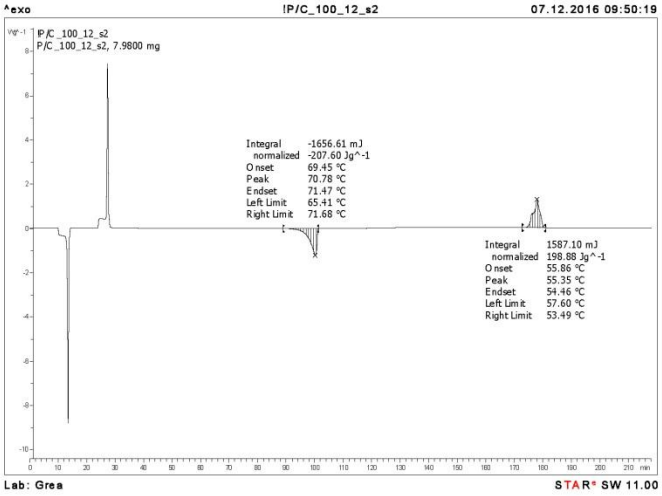


**Figure 32.** DSC response and evaluation of dodecyl DHSE. Cycled sample 2. 100 cycles.

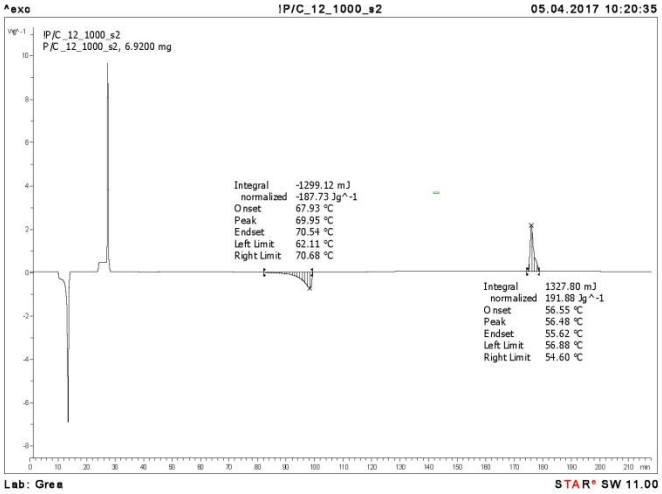


**Figure 33.** DSC response and evaluation of dodecyl DHSE. Cycled sample 1. 1000 cycles.

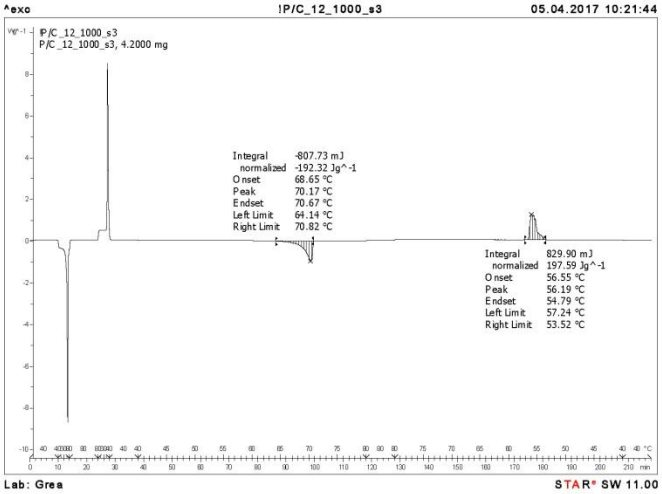


**Figure 34.** DSC response and evaluation of dodecyl DHSE. Cycled sample 2. 1000 cycles.

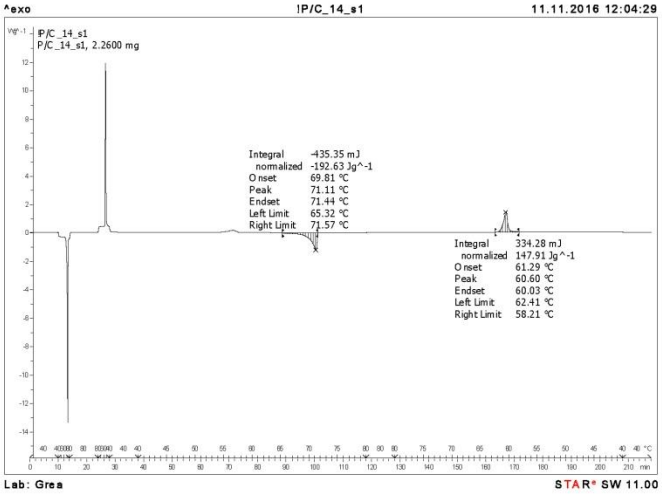


**Figure 35.** DSC response and evaluation of tetradecyl DHSE. Not cycled sample 1.

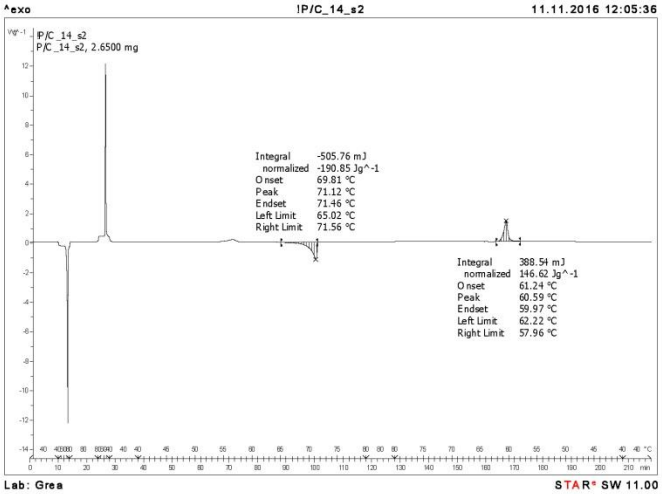


**Figure 36.** DSC response and evaluation of tetradecyl DHSE. Not cycled sample 2.

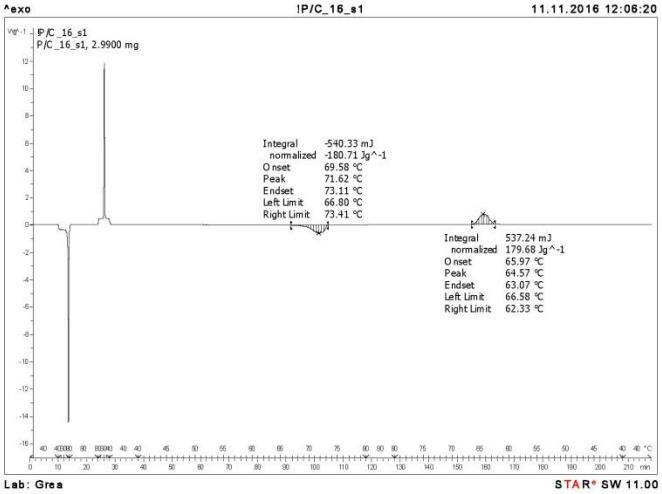


**Figure 37.** DSC response and evaluation of hexadecyl DHSE. Not cycled sample 1.

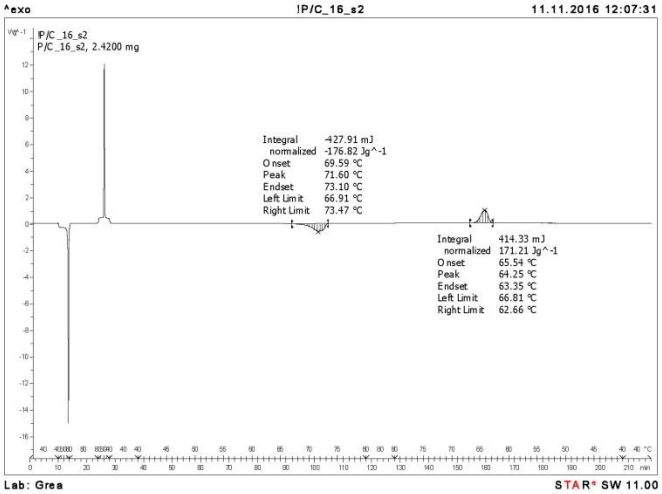


**Figure 38.** DSC response and evaluation of hexadecyl DHSE. Not cycled sample 2.

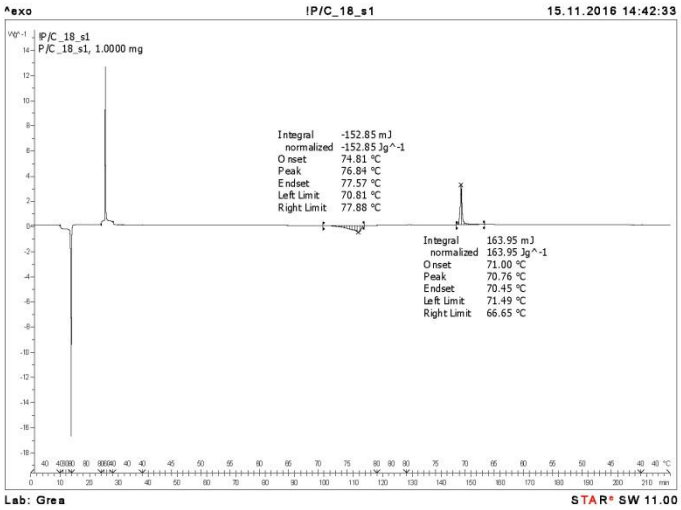


**Figure 39.** DSC response and evaluation of octadecyl DHSE. Not cycled sample 1.

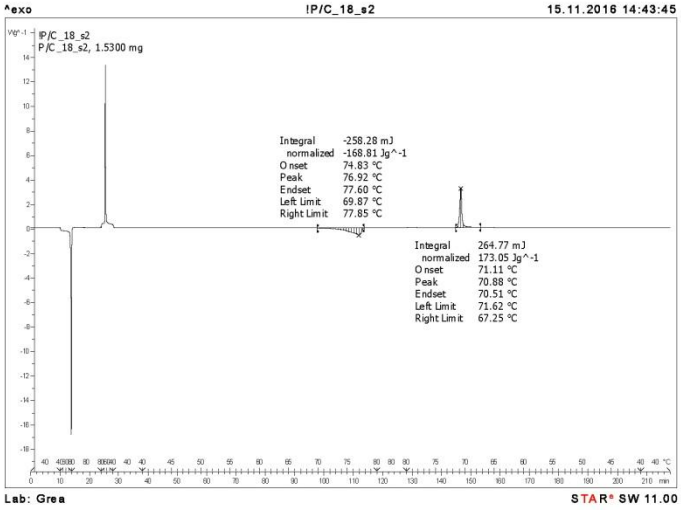


**Figure 40.** DSC response and evaluation of octadecyl DHSE. Not cycled sample 2.

## *$^{1}$H NMR Spectra of the products prepared*

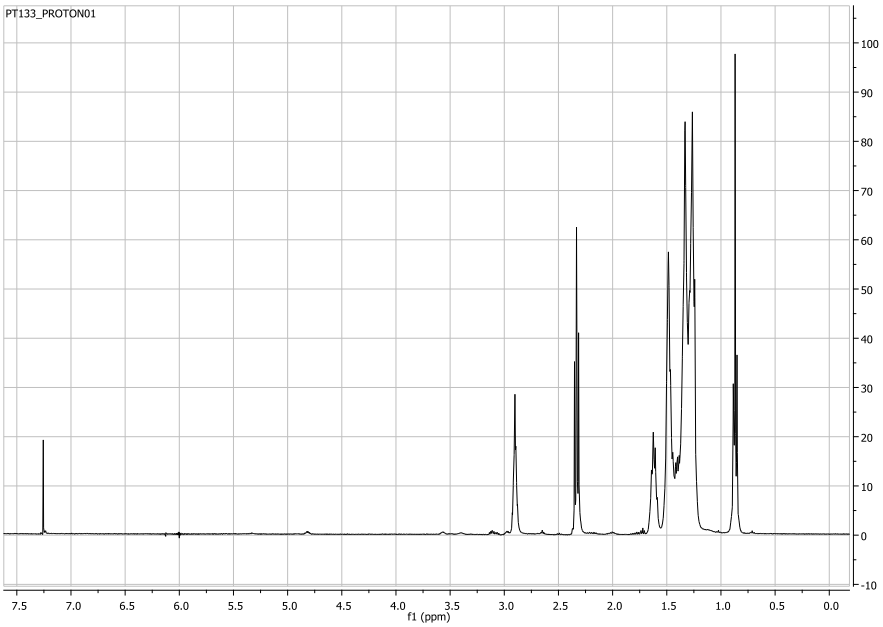


***Figure 41.*** *$^{1}$H NMR Spectra of the cis-9, 10-epoxyestearic acid.*

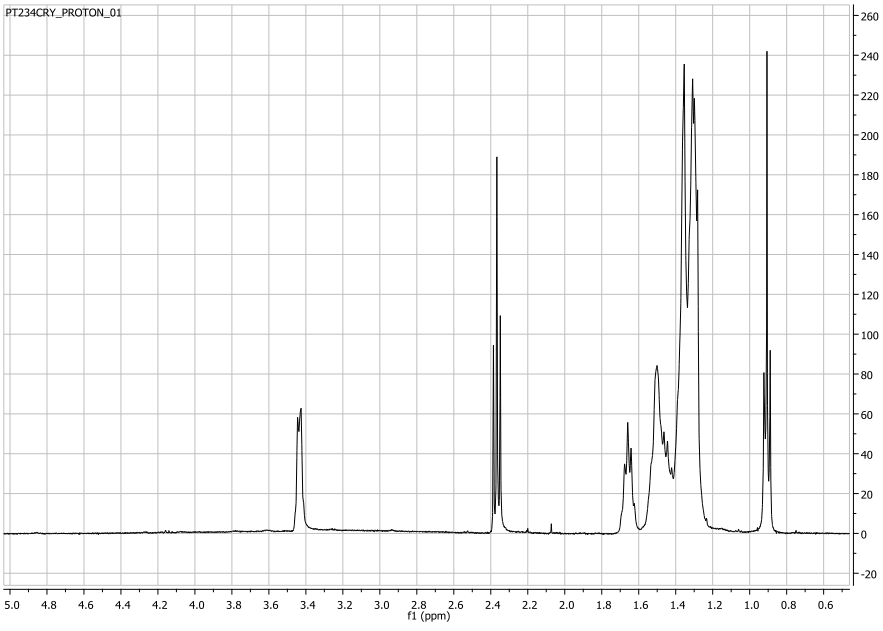


***Figure 42.*** *$^{1}$H NMR Spectra of the DHSA.*

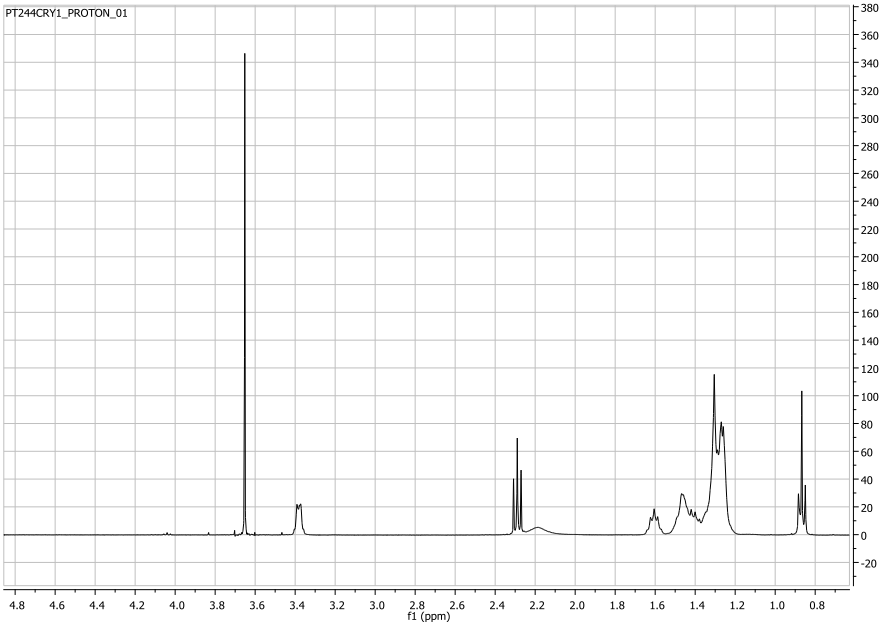


***Figure 43.*** *$^{1}$H NMR Spectra of the methyl DHSE.*

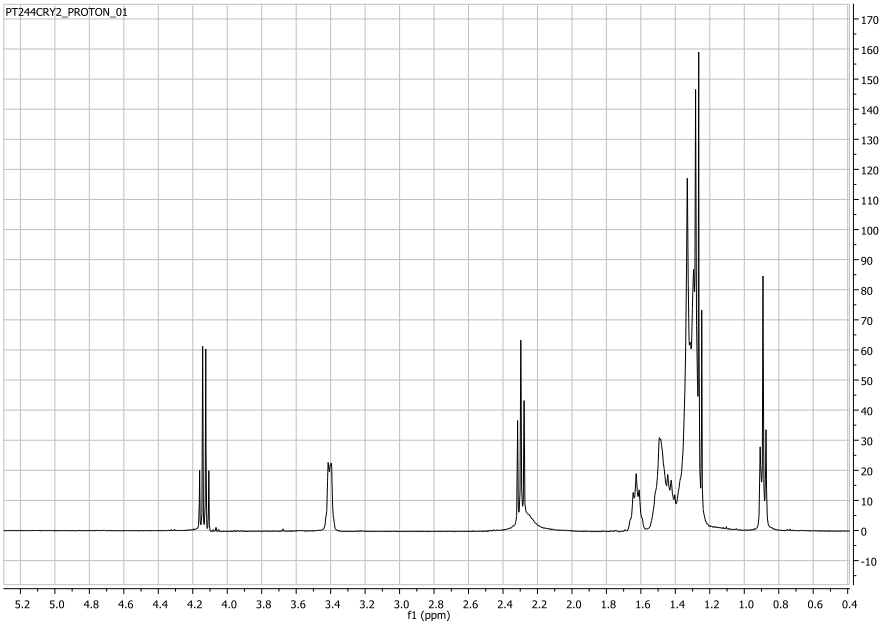


***Figure 44.*** *$^{1}$H NMR Spectra of the ethyl DHSE.*

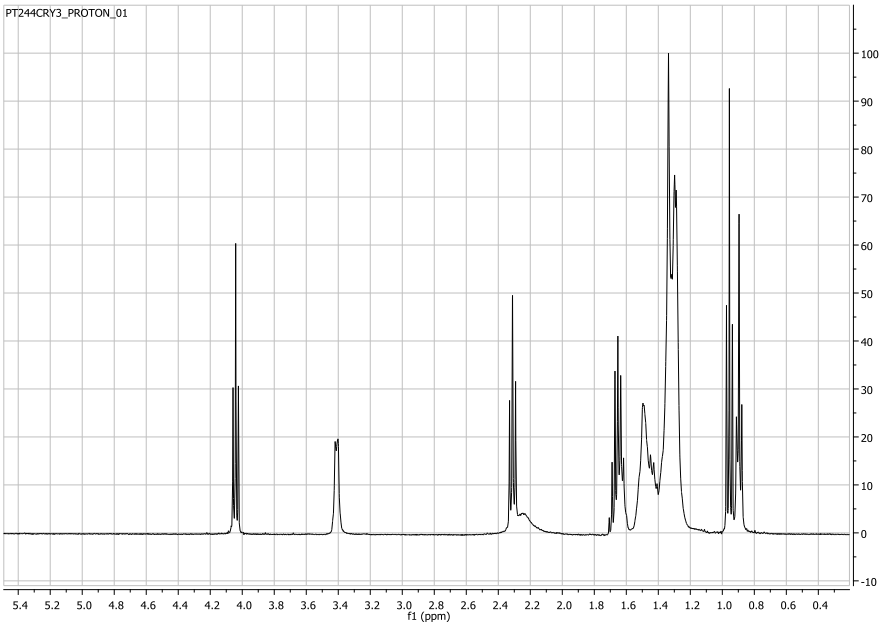


***Figure 45.*** *$^{1}$H NMR Spectra of the propyl DHSE.*

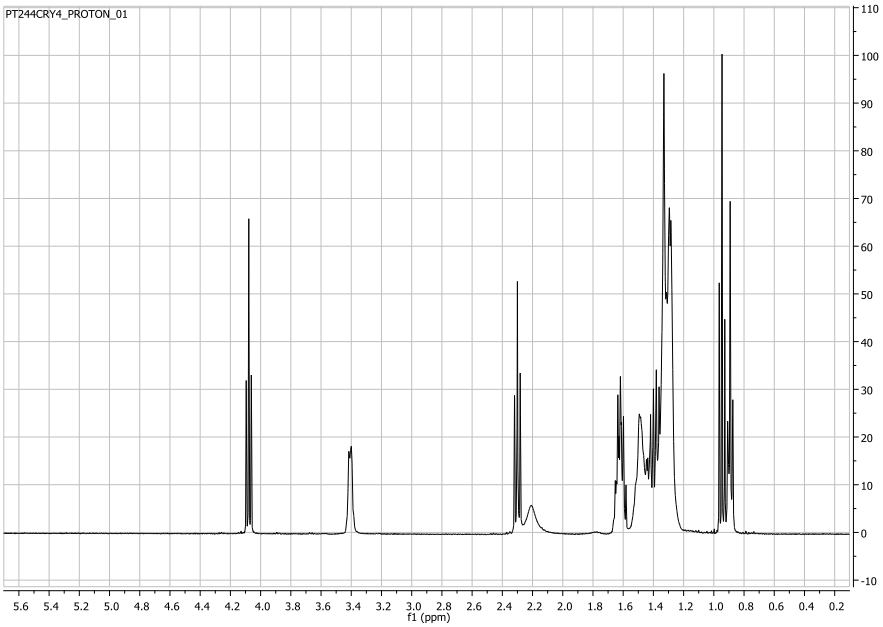


***Figure 46.*** *$^{1}$H NMR Spectra of the butyl DHSE.*

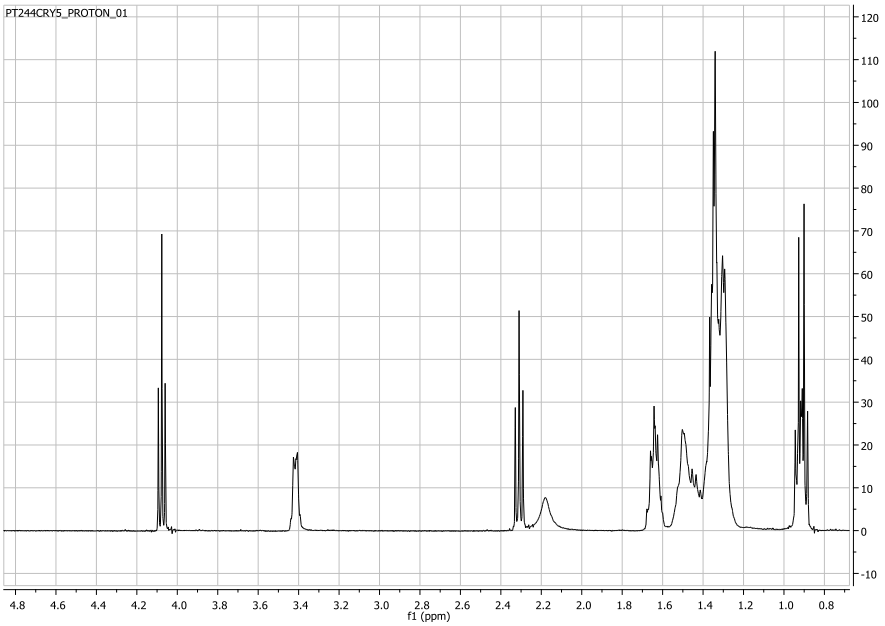


***Figure 47.*** *$^{1}$H NMR Spectra of the pentyl DHSE.*

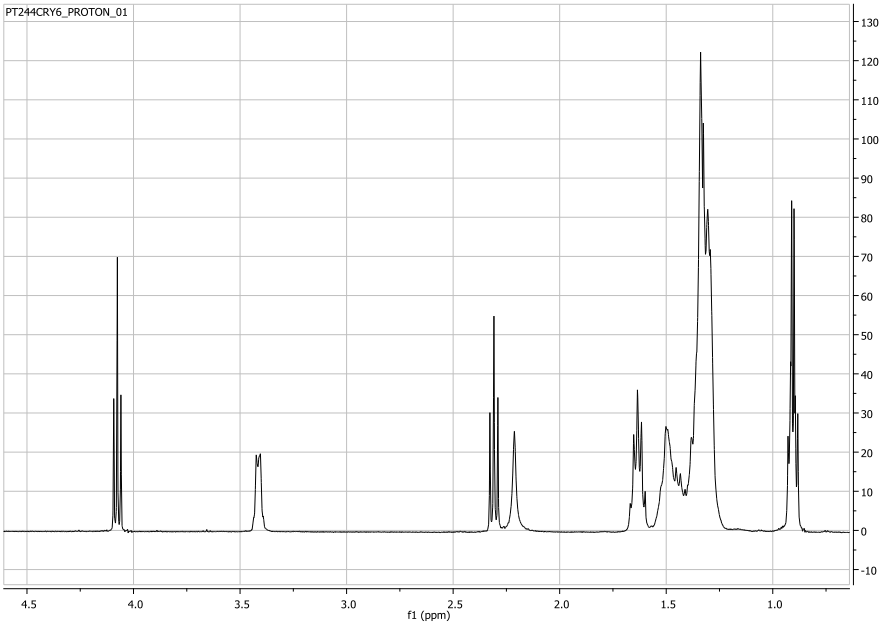


***Figure 48.*** *$^{1}$H NMR Spectra of the hexyl DHSE.*

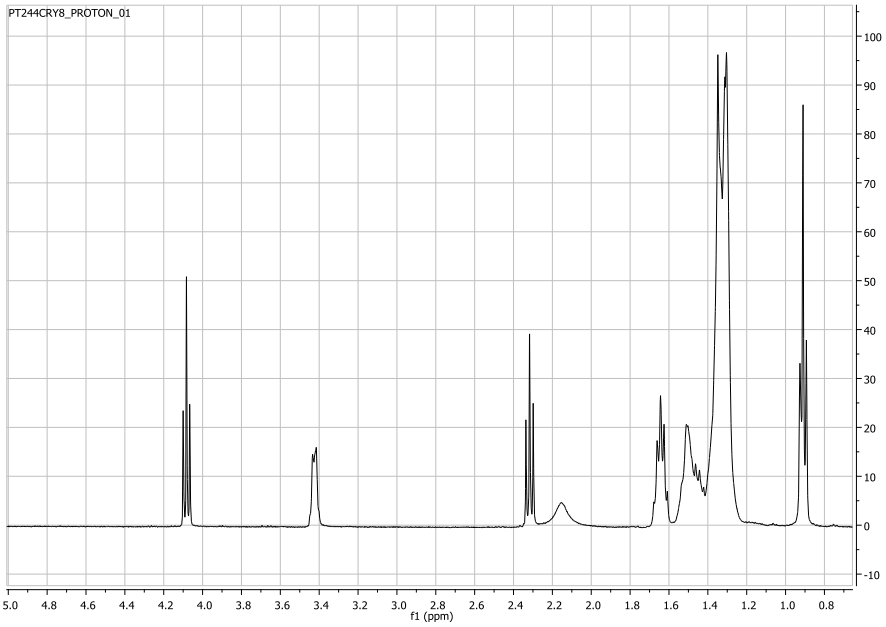


***Figure 49.*** *$^{1}$H NMR Spectra of the octyl DHSE.*

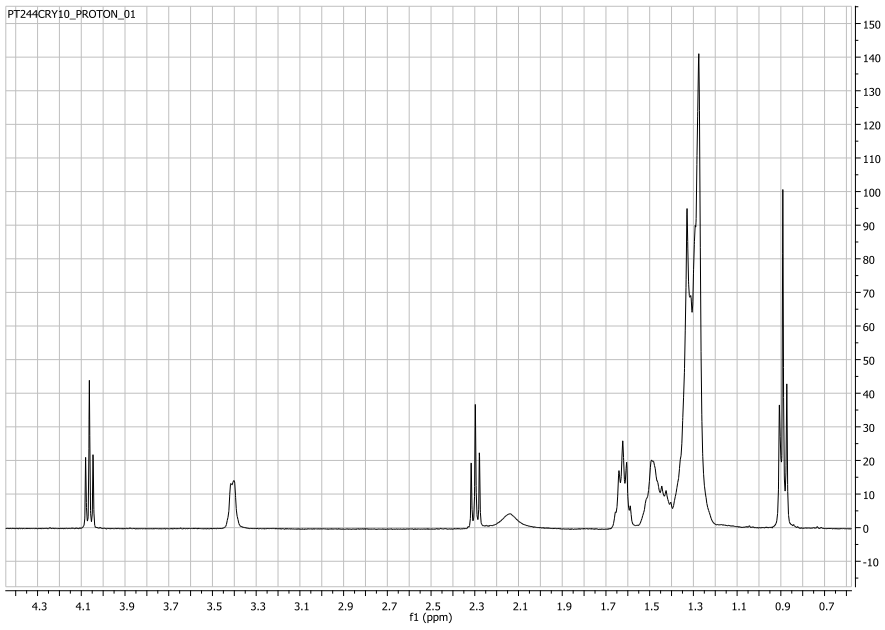


***Figure 50.*** *$^{1}$H NMR Spectra of the decyl DHSE.*

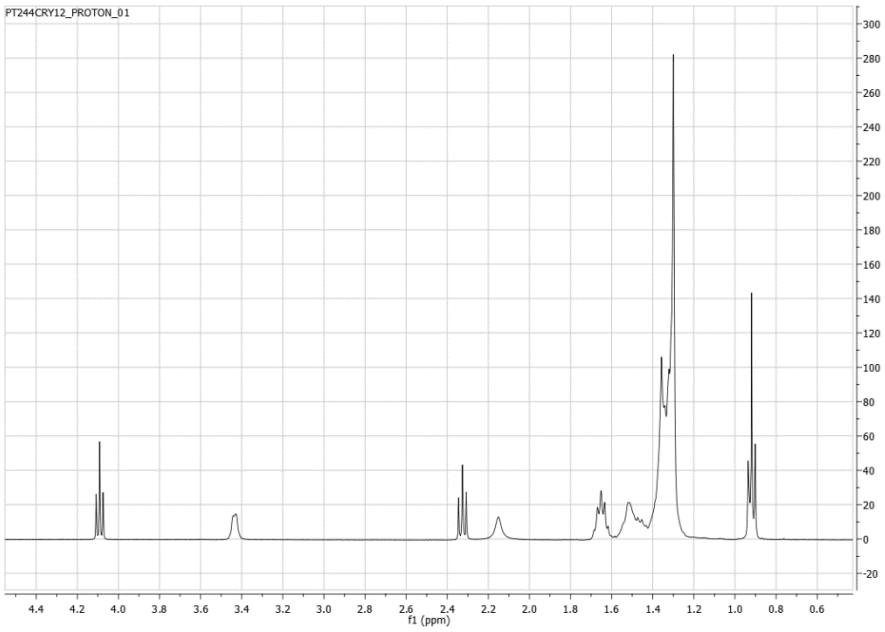


***Figure 51.*** *$^{1}$H NMR Spectra of the dodecyl DHSE.*

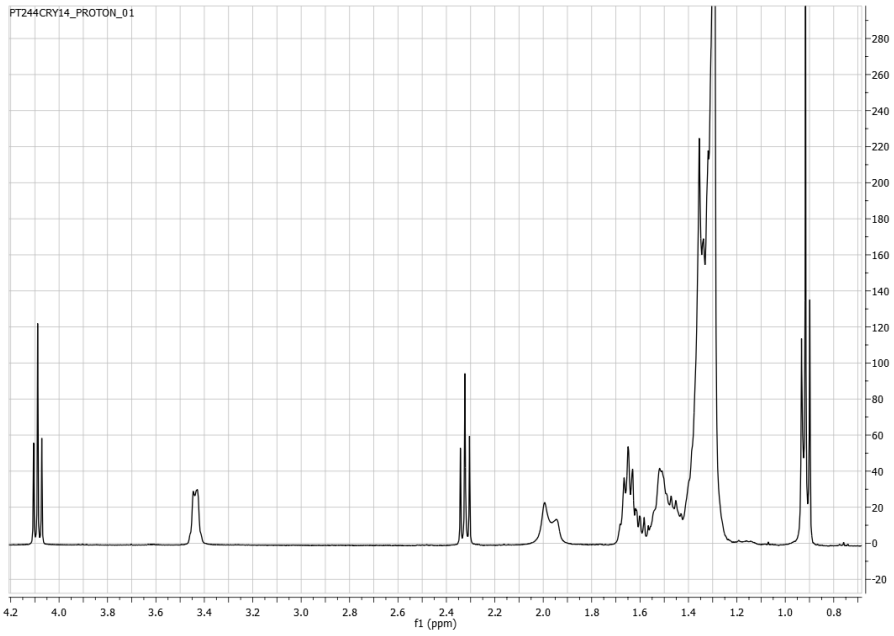


***Figure 52.*** *$^{1}$H NMR Spectra of the tetradecyl DHSE.*

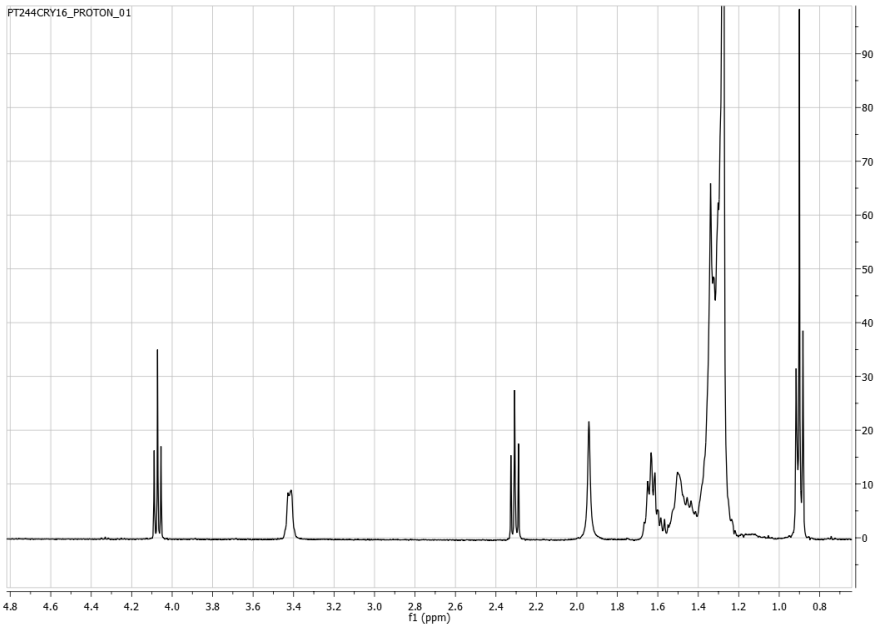


***Figure 53.*** *$^{1}$H NMR Spectra of the hexadecyl-DHSE.*

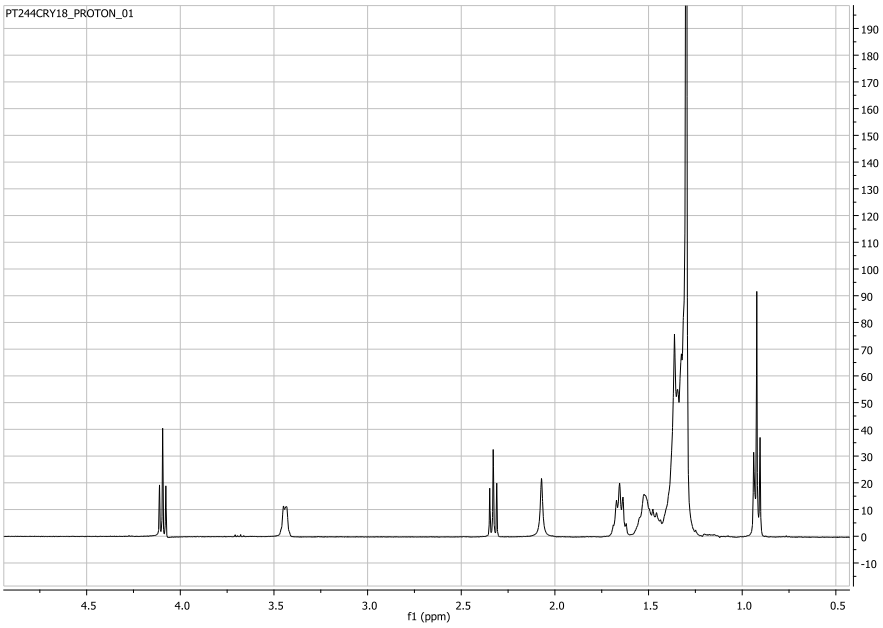


***Figure 54.*** *$^{1}$H NMR Spectra of the octadecyl DHSE.*